

TYPE Ia SUPERNOVAE AND THE HUBBLE CONSTANT

David Branch

Department of Physics and Astronomy, University of Oklahoma, Norman, Oklahoma
73019; e-mail: branch@mail.nhn.ou.edu

KEY WORDS: cosmology, white dwarf

ABSTRACT

The focus of this review is the work that has been done during the 1990s on using Type Ia supernovae (SNe Ia) to measure the Hubble constant (H_0). SNe Ia are well suited for measuring H_0 . A straightforward maximum-light color criterion can weed out the minority of observed events that are either intrinsically subluminal or substantially extinguished by dust, leaving a majority subsample that has observational absolute-magnitude dispersions of less than $\sigma_{\text{obs}}(M_B) \simeq \sigma_{\text{obs}}(M_V) \simeq 0.3$ mag. Correlations between absolute magnitude and one or more distance-independent SN Ia or parent-galaxy observables can be used to further standardize the absolute magnitudes to better than 0.2 mag. The absolute magnitudes can be calibrated in two independent ways: empirically, using Cepheid-based distances to parent galaxies of SNe Ia, and physically, by light curve and spectrum fitting. At present the empirical and physical calibrations are in agreement at $M_B \simeq M_V \simeq -19.4$ or -19.5 . Various ways that have been used to match Cepheid-calibrated SNe Ia or physical models to SNe Ia that have been observed out in the Hubble flow have given values of H_0 distributed throughout the range of $54\text{--}67$ km s $^{-1}$ Mpc $^{-1}$. Astronomers who want a consensus value of H_0 from SNe Ia with conservative errors could, for now, use 60 ± 10 km s $^{-1}$ Mpc $^{-1}$.

1. INTRODUCTION

One way to illustrate the rapid progress in using Type Ia supernovae (SNe Ia) for cosmology is to compare the situation now with that of six years ago when the article “Type Ia Supernovae as Standard Candles” (Branch & Tammann 1992) appeared in this series of reviews. At that time, optimism was expressed about checking that light curves of SNe Ia are time-dilated, as they should be if

the universe really is expanding; about using SNe Ia to measure galaxy peculiar velocities; and about using them to determine the cosmic deceleration—but hardly any significant results on these matters were at hand. Now, thanks to the exertions of supernova (SN) observers, the time dilation has been established (Goldhaber et al 1997, Leibundgut et al 1996, Riess et al 1997b); peculiar motions are beginning to be estimated (Riess et al 1995b, 1997a, Hamuy et al 1996b); and above all, estimates of the matter-density parameter Ω_m and the cosmological-constant contribution Ω_Λ are beginning to be made (Perlmutter et al 1997a, 1998, Garnavich et al 1998). All of this work entails using SNe Ia as precise indicators of *relative* distances in a purely empirical way. Dramatic progress is being made on these matters, but at this time a review article would be premature.

A competitive measurement of the Hubble constant (H_0), on the other hand, requires *absolute* distances but less precision. Traditionally, those who have used SNe Ia to estimate H_0 have obtained values that have been, in the context of the longstanding distance-scale controversy, low values. For example, before Cepheid variables in any SN Ia parent galaxy had been discovered Branch & Tammann (1992) offered $H_0 = 57 \pm 7 \text{ km s}^{-1} \text{ Mpc}^{-1}$. (The units of H_0 will not be repeated.) Within the last six years, so much has been said and done about obtaining the value of H_0 from SNe Ia that this alone is the topic of this review.

Most of the literature citations are from the 1990s. Many earlier ones that are now mainly of historical interest can be found in the review by Branch & Tammann (1992). For a recent comprehensive collection of articles on practically all aspects of SN Ia research, see *Thermonuclear Supernovae*, edited by Ruiz-Lapuente et al (1997b), and for a recent collection of articles on various ways to estimate H_0 , see *The Extragalactic Distance Scale*, edited by Livio et al (1997).

Sections 2 and 3 focus on empirical matters, with the former devoted to the observational properties of SNe Ia and the latter to the determination of H_0 by means of Cepheid-based calibrations of SN Ia absolute magnitudes. Then the physical properties of SNe Ia are discussed in Section 4, and the determination of H_0 by physical methods is the subject of Section 5. Section 6 states the conclusion.

2. OBSERVATIONAL PROPERTIES OF SNE Ia

Among the observational advances of recent years, some of the highlights have been as follows.

Several SNe Ia in relatively nearby galaxies have been well observed. Normal events include SN 1989B in NGC 3627 of the Leo group of galaxies (Barbon et al 1990, Wells et al 1994), SN 1990N in NGC 4639 of the Virgo complex

(Leibundgut et al 1991a, Jeffery et al 1992, Mazzali et al 1993), SN 1992A in NGC 1380 of the Fornax cluster (Kirshner et al 1993, Hamuy et al 1996d), and SN 1994D in NGC 4526 in Virgo (Richmond et al 1995, Patat et al 1996, Meikle et al 1996, Vacca & Leibundgut 1996). The two most notoriously peculiar events, SN 1991T in NGC 4527 (Ruiz-Lapuente et al 1992, Filippenko et al 1992a, Phillips et al 1992, Jeffery et al 1992, Mazzali et al 1995) and SN 1991bg in NGC 4374 (Filippenko et al 1992b, Leibundgut et al 1993, Turatto et al 1996, Mazzali et al 1997), were in the Virgo complex. SN 1986G in NGC 5128 \equiv Centaurus A (Phillips et al 1987, Cristiani et al 1992) also was peculiar, in the sense of SN 1991bg but less extreme. It is noteworthy that some of these events were discovered closer to their times of explosion than to their times of maximum light, that ultraviolet spectra of SN 1992A were obtained by the Supernova Intensive Study (SINS) collaboration using the *Hubble Space Telescope* (HST) (Kirshner et al 1993), and that infrared spectra of SN 1994D (Meikle et al 1996) and several other SNe Ia (Bowers et al 1997) have been observed.

Accurate CCD light curves have been measured for dozens of SNe Ia out in the Hubble flow ($z > 0.01$), where the recession velocities of their parent galaxies should be reliable indicators of their relative distances. The discovery and photometry of such events have been accomplished mainly by the Calán-Tololo collaboration (Hamuy et al 1993, 1995b, 1996c; see also Riess 1996).

SNe Ia at high redshift by SN standards, $z > 0.3$, are being discovered in even larger numbers (Perlmutter et al 1997b,c, Schmidt et al 1997). *Scheduled* discoveries of whole batches of such events have become routine (which is not to say easy), thus allowing the opportunity for follow-up spectroscopy and photometry to be arranged in advance. The primary purpose of the search for high- z SNe Ia is to use them as indicators of relative distances for the determination of Ω_m and Ω_Λ , but they also have been used to constrain the ratio of the global and local values of H_0 to be near (Kim et al 1997, Tripp 1997) but perhaps slightly less than (Zehavi et al 1998) unity.

2.1 *Homogeneity and Diversity*

Much has been written, pro and con, about the observational homogeneity of SNe Ia, and for the most part the discussion has followed a natural course. Before the 1990s and even in 1992 (Branch & Tammann 1992), when most of the mild apparent differences among SNe Ia were comparable to the observational errors, the striking observational homogeneity was emphasized, although it already was clear both photometrically (Phillips et al 1987) and spectroscopically (Branch et al 1988) that SNe Ia are not strictly homogeneous. After the discovery of the obviously deviant SNe 1991T and 1991bg, it became necessary to split SNe Ia into a majority of normal events and a minority of peculiar ones.

In the 1990s, the observational data have improved so much that it has become possible to look seriously at the diversity even among normal SNe Ia. This has brought about a natural new emphasis on the diversity—but it would be a mistake to lose sight of the fact that even as the new data have illuminated the diversity, they also have confirmed that *normal SNe Ia are highly homogeneous*. When made in the context of using SNe Ia to determine H_0 , statements such as “SNe Ia are far from standard candles” and “the concept of a normal SN Ia is without merit” do more to obscure than to illuminate the reality.

It is clear and uncontroversial that events like SN 1991bg and to a lesser extent SN 1986G are “weak” explosions. They can be readily distinguished from normal SNe Ia on the basis of practically any spectroscopic or photometric observable, so although they are very interesting physically, they need have no bearing on the determination of H_0 . Even if these intrinsically red, dim events did not exist, we would still have to deal with red, dim, extinguished events. Coping with events like SN 1991T is less straightforward, but they are uncommon and do not pose a serious problem for H_0 . In the rest of this section we consider the distributions of various observational properties of SNe Ia, with some emphasis on the extent to which the normal events are homogeneous and diverse.

2.1.1 SPECTRA Observational aspects of SN spectra and their classification have been reviewed in this series by Filippenko (1997). Given a decent spectrum, deciding whether an event is or is not a Type Ia is practically always unambiguous (except at high redshift). Spectra of three normal SNe Ia and the peculiar SNe 1991T, 1991bg, and 1986G, all near maximum light, are displayed in the *right panel* of Figure 1 (see Section 4.4 for discussion of the *left panel*). Normal SNe Ia undergo a characteristic spectral evolution, showing P Cygni lines of Si II, Ca II, S II, O I, and Mg II prior to and near maximum light, developing blends of P Cygni permitted Fe II lines shortly thereafter, and finally developing blends of forbidden emission lines of iron and cobalt ions during the late nebular phase. The most conspicuous spectroscopic peculiarity of weak events like SNe 1991bg and 1986G during their photospheric phase is that they show a broad absorption trough around 4200 Å, produced by low-excitation Ti II lines (Filippenko et al 1992a). In SN 1991T, prior to and around maximum light, high-excitation lines of Fe III were prominent (Ruiz-Lapuente et al 1992, Filippenko et al 1992b). By a few weeks after maximum light, the spectra of SN 1991T looked nearly normal.

Looking at line spectra is a good way to study diversity because the strengths and blueshifts of the lines (in the SN rest frame) are not affected by extinction or distance. In terms of the general appearance of their spectral features, most SNe Ia look very similar. For a beautiful illustration of what is meant by SN Ia

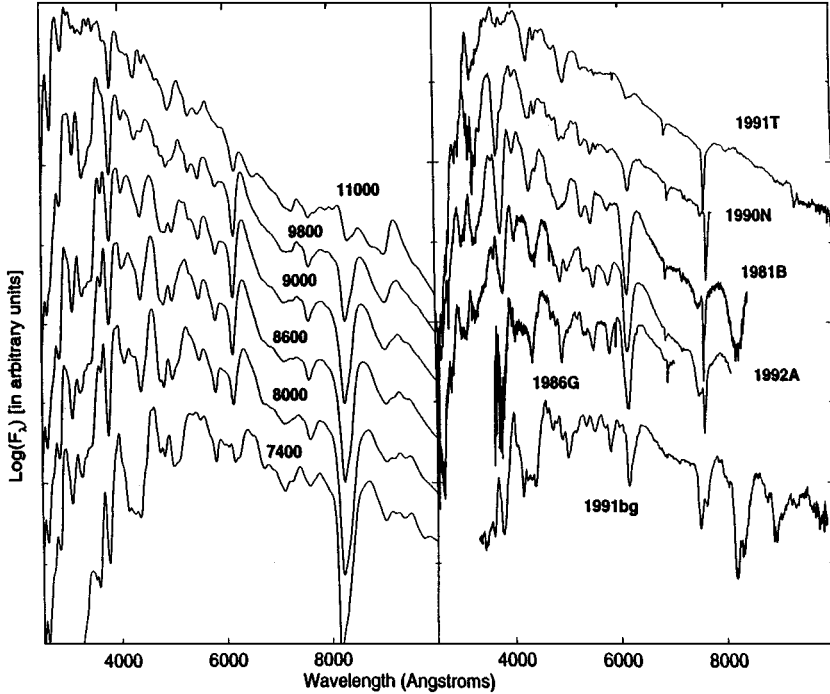


Figure 1 Nonlocal thermodynamic equilibrium (NLTE) spectra calculated for the composition structure of model W7, 15 days after explosion and a range of effective temperatures (*left*), and observed spectra of SNe Ia near maximum light (*right*). From Nugent et al (1995c).

spectral homogeneity, see figure 6 of Filippenko (1997). Branch et al (1993) defined what they meant by spectroscopically normal (like SNe 1981B, 1989B, 1992A, and 1972E) and peculiar (like SNe 1986G, or 1991bg, or 1991T) and then found that 83 to 89% of the SNe Ia whose spectra they were able to subclassify were normal. Subtle differences in the spectra of normal SNe Ia were nevertheless evident. As more SN Ia spectra have been published [Gómez et al (1996) set a record by presenting spectra of 27 different SNe Ia in one paper], the situation has not changed: Most SNe Ia in the observational sample are spectroscopically normal in the sense of Branch et al (1993).

Spectroscopic diversity can be quantified by measuring blueshifts of absorption features or monochromatic flux ratios. Branch & van den Bergh (1993) compiled data on the wavelength of the absorption minimum near 6100 Å during the photospheric phase of 36 SNe Ia and converted to velocity on the assumption that the feature is produced by blueshifted $\lambda 6355$ of Si II. It should

be noted that Fisher et al (1997) suggested that in pre-maximum spectra, this absorption feature may be partially produced by $\lambda 6580$ of C II; if this is correct, then some of the velocities derived on the basis of the Si II identification will need to be revised. In any case the measured differences in the feature wavelength at a given phase exceed the observational uncertainties. Branch & van den Bergh (1993) defined a parameter $V_{10}(\text{Si})$, the blueshift at 10 days after maximum light (late enough to be unaffected by C II). SNe Ia have $8,000 < V_{10}(\text{Si}) < 14,000 \text{ km s}^{-1}$. Weak SNe Ia tend to have the very lowest values, but there also are definite differences among normal SNe Ia.

For a small sample of 12 SNe Ia, Fisher et al (1995) defined a parameter $V_R(\text{Ca})$ that is based on the wavelength of the red edge of the Ca II H&K absorption feature at moderately late times and intended as a measure of the minimum ejection velocity of calcium. The weak SNe 1991bg and 1986G had exceptionally low $V_R(\text{Ca})$ values, 1600 and 2700 km s^{-1} , respectively, while normal SNe Ia had $4000 < V_R(\text{Ca}) < 7300 \text{ km s}^{-1}$. For a sample of 8 SNe Ia, Nugent et al (1995c) defined parameters $R(\text{Si})$, based on the relative depths at maximum light of the Si II absorption features near 5800 and 6150 Å, and $R(\text{Ca})$, based on the relative heights of the emission peaks on both sides of the Ca II H&K absorption feature. Again, SN 1991bg and to a lesser extent SN 1986G had extreme values of both parameters, and clear differences were observed among the normal SNe Ia.

Thus, on the basis of the general appearance of their spectra, SNe Ia can be divided into a majority of normals and a minority of peculiars. When spectral features are quantified, peculiar weak events have extreme values of the parameters. Moderate spectral diversity among normal SNe Ia also exists, and given good data, it can be quantified in various ways.

2.1.2 LIGHT-CURVE SHAPES Like spectra, rest-frame light-curve shapes are independent of distance and of extinction (to first order). And like SN Ia spectra, SN Ia light-curve shapes are impressively homogeneous (Hamuy et al 1991, Leibundgut et al 1991b, Branch & Tammann 1992). The first obviously deviant light curves were those of SN 1986G (Phillips et al 1987), which was fast, and SN 1991bg (Filippenko et al 1992a, Leibundgut et al 1993), which was faster. Now that good photometry is available for numerous SNe Ia, more moderate differences among light curves can be studied. The parameter that most often has been used to quantify light-curve shapes is Δm_{15} (Phillips 1993), the magnitude decline in the B band during the first 15 days after maximum light. Often, when the data for a direct measurement of Δm_{15} are not available, a value is assigned by fitting the data to template light curves of SNe Ia having various values of Δm_{15} . Hamuy et al (1996d) presented a set of six templates in the B , V , and I bands, ranging from the rather slow light curves of SNe

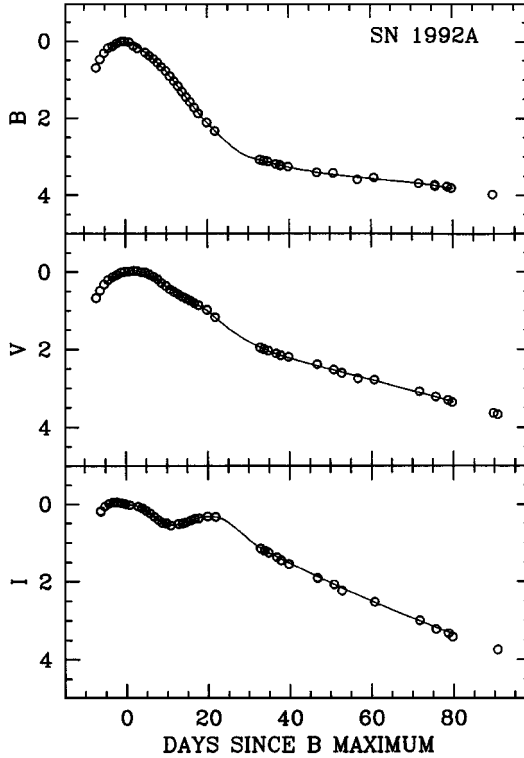


Figure 2 Light curves of SN 1992A. From Hamuy et al (1996d).

1992bc ($\Delta m_{15} = 0.87$) and 1991T ($\Delta m_{15} = 0.94$) to the very rapid ones of SN 1991bg ($\Delta m_{15} = 1.93$). The SN 1992A light curves ($\Delta m_{15} = 1.47$) are shown in Figure 2 as an example of superb photometric data, and a comparison of the shapes of the six templates is shown in Figure 3. Light-curve shape diversity exists, and given good data, it can be quantified.

2.1.3 COLORS AND ABSOLUTE MAGNITUDES Colors and absolute magnitudes are both affected by interstellar extinction, so I discuss them together. A source of confusion in the past was that a few SNe Ia were reported to be very blue at maximum light, with $B - V \simeq -0.3$. (Throughout this article $B - V$ is the difference between the peak B and peak V values, i.e. it is really $B_{\max} - V_{\max}$.) This implied either a wide range in intrinsic color among normal SNe Ia or a characteristic very blue intrinsic color with considerable interstellar reddening as the norm rather than the exception. However, CCD photometry

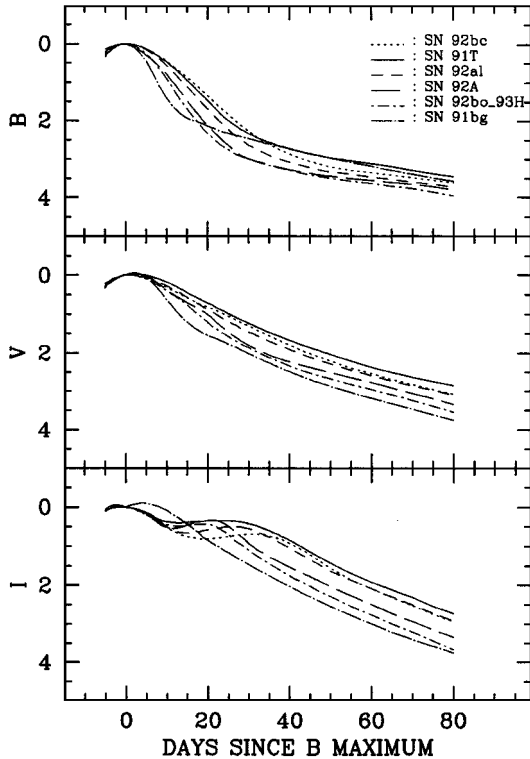


Figure 3 Comparison of six light-curve templates. From Hamuy et al (1996d).

of comparison stars that were used for the old photographic photometry has confirmed a previous suspicion that the “too-blue” colors were in error (Patat et al 1997), and now the color distribution of SNe Ia is strongly peaked near $B - V = 0$. The minority of events that have much redder values include some like SN 1989B ($B - V = 0.35$), which were intrinsically normal but obviously reddened by dust, and weak events like SN 1991bg ($B - V = 0.87$), which were intrinsically red. That most SNe Ia should escape severe extinction in their parent galaxies is not surprising (Hatano et al 1998). In addition, of course, observational selection works against the discovery and follow-up of the small fraction of SNe Ia that do happen to be severely extinguished.

For the distribution of peak absolute magnitudes, relative distances are required. On the basis of a sample that included data from Hamuy et al (1995b) as well as some earlier less accurate data, Vaughan et al (1995) and Tammann & Sandage (1995) stressed that when a simple $B - V$ criterion is used to exclude

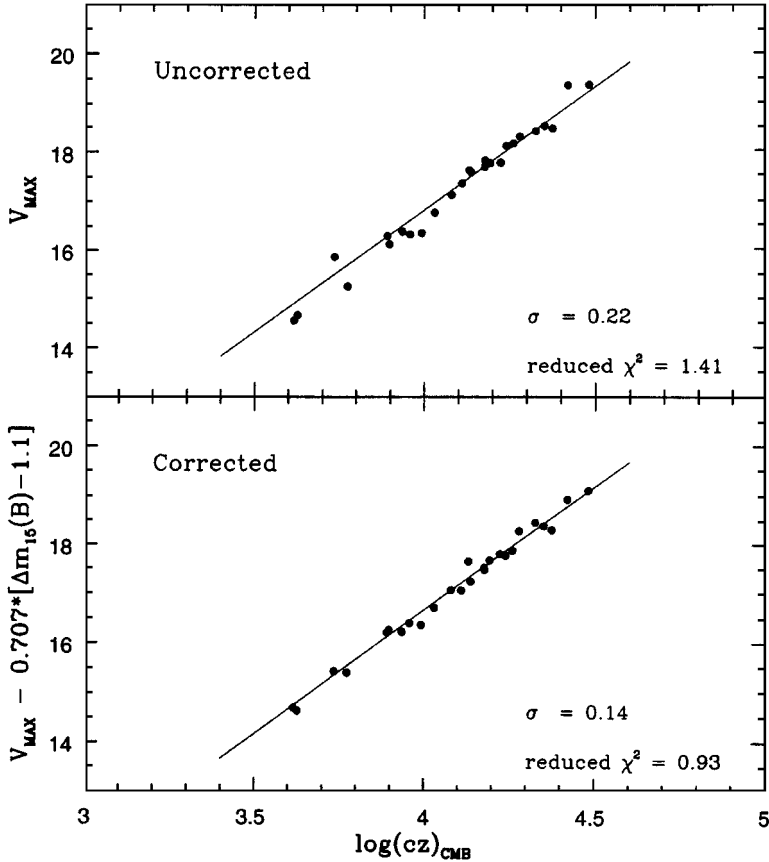


Figure 4 The Hubble diagram in V for the 26 SNe Ia in the Calán-Tololo sample having $B - V \leq 0.20$ (top), and after correction for a magnitude-decline correlation (bottom). From Hamuy et al (1996b).

SNe Ia that are observationally red, whether intrinsically or because of dust, one is left with a sample of nearly standard candles. This has been confirmed by Hamuy et al (1996b). The *top panel* of Figure 4 shows the Hubble diagram in V for the 26 events in their sample having $B - V < 0.2$ (see Section 2.2 for discussion of the *bottom panel*). The observational absolute-magnitude dispersions of these events are only $\sigma_{\text{obs}}(M_B) = 0.24$, $\sigma_{\text{obs}}(M_V) = 0.22$, and $\sigma_{\text{obs}}(M_I) = 0.19$. Applying a color cut is a very straightforward strategy for obtaining a sample of nearly standard candles, but it can be misunderstood (von Hippel et al 1997). The mean absolute magnitudes, corrected for Galactic

but not parent-galaxy extinction, of the 26 events of Hamuy et al (1996b) that pass the color cut are

$$M_B \simeq M_V \simeq -19.30 (\pm 0.03) + 5 \log (H_0/60). \quad (1)$$

Saha et al (1997) show a Hubble diagram (their figure 10) for a larger sample of 56 SNe Ia that includes some more recent data (Riess 1996) but also some older data that are not as precise as those of Hamuy et al (1996b); therefore, the dispersions for the Saha et al sample are somewhat higher, $\sigma_{\text{obs}}(M_B) = 0.33$ and $\sigma_{\text{obs}}(M_V) = 0.31$. Wang et al (1997a) point out that the scatter in the absolute magnitudes, uncorrected for extinction, of SNe Ia beyond about 7.5 kpc from the centers of their parent galaxies is very small; unfortunately, none of the Cepheid-calibrated SNe Ia discussed in Section 3 were that far out.

Figure 5 shows absolute magnitude plotted against $B - V$ for the Calán-Tololo sample. For the entire sample, including the weak SN 1992K that resembled SN 1991bg (Hamuy et al 1995a), the weak 1993H that probably was like SN 1986G (Hamuy et al 1996b), and the moderately extinguished SN 1990Y (Hamuy et al 1995), a correlation is obvious, and even when the three red events are excluded a correlation remains. In the past, the correlation between color and absolute magnitude seemed to require that the extinction characteristics of the dust that reddens SNe Ia in external galaxies differ from those of the dust in our Galaxy (Branch & Tammann 1992 and references therein). Recently this problem has been thought to have been due to the old “too-blue” SNe Ia mentioned above and to the adoption of a single intrinsic value of $B - V$ for SNe Ia (Della Valle & Panagia 1992, Sandage & Tammann 1993, Vaughan et al 1995, Riess et al 1996b). Strangely enough, the mystery appears to have resurfaced (Tripp 1998).

2.2 Correlations

Here we consider correlations between observables other than the one just discussed between color and absolute magnitude. As stressed above, weak events like SN 1991bg are extreme in many of their properties, so when normal and weak SNe Ia are considered together, correlations are obvious. The more interesting issue is the extent to which correlations hold among normal SNe Ia. First we consider those among distance-independent observables.

It is clear that there is a correlation between spectrum and light-curve shape. Nugent et al (1995c) found that the spectroscopic observables $R(\text{Ca})$ and $R(\text{Si})$ correlate well with the light-curve decline rate Δm_{15} . Therefore the concept of a one-dimensional photometric/spectroscopic sequence is useful. The situation is not really that simple, though. For example, some events whose spectra look normal in the sense of Branch et al (1993) do not fit into a one-dimensional sequence in terms of the Si II blueshifts studied by Branch & van den Bergh

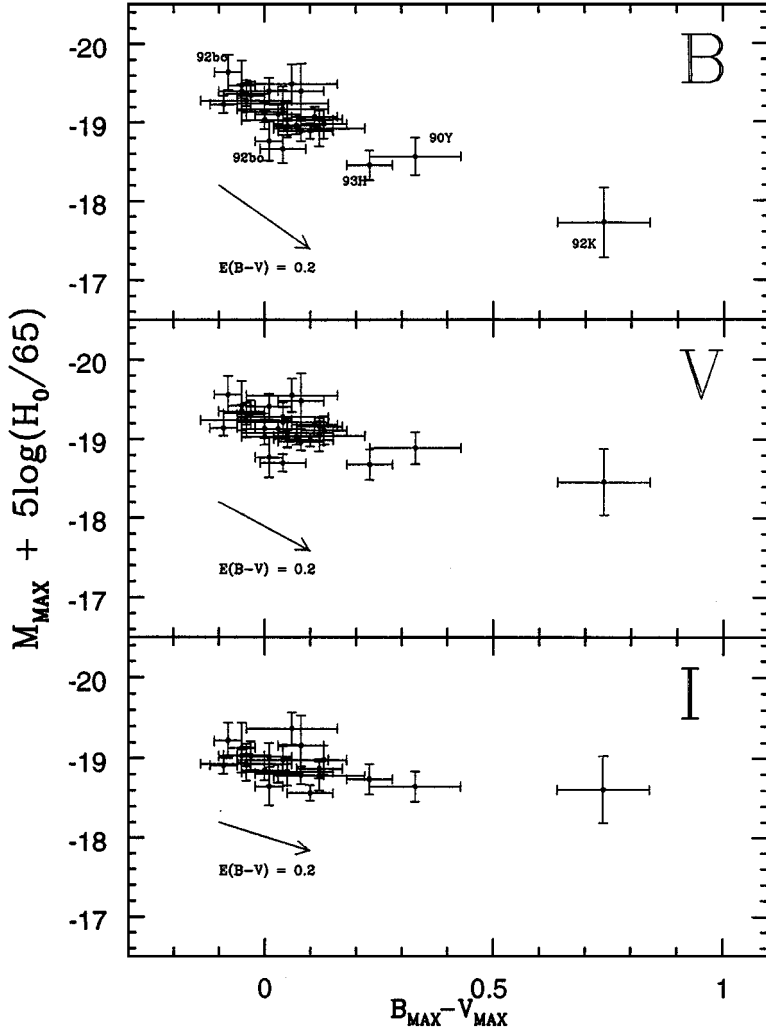


Figure 5 Absolute magnitudes of the Calán-Tololo sample are plotted against $B - V$. The extinction vectors have conventional slopes of 4.1 in B , 3.1 in V , and 1.85 in I . From Hamuy et al (1996b).

(1993). SNe 1983G and 1984A had normal looking spectra but exceptionally high $V_{10}(\text{Si})$ values. Similarly, Hamuy et al (1996d) found that although in general their light-curve templates can be arranged in a one-dimensional sequence from slow to fast, some light curves having very similar initial decline rates show significant differences of detail. SN 1994D had an anomalously negative $U - B$ color for its decline rate. And although SN 1992bc had a slower light curve than the spectroscopically peculiar SN 1991T, SN 1992bc had a normal looking spectrum. This and other evidence suggest that events like SN 1992bc may represent the “strong” end of the sequence of normals, while SN 1991T and similar events that have been discovered recently comprise a separate subgroup of powerful SNe Ia, which may be super-Chandrasekhar products of white-dwarf mergers in young populations (see Section 4.4).

Looking for correlations between $B - V$ and other distance-independent observables is difficult because for all but the weak SNe Ia, the intrinsic $B - V$ distribution is so strongly peaked near zero. The $U - B$ color appears to cover more of a range than $B - V$ (Schaefer 1995b) and to be correlated with other SN Ia properties (Branch et al 1997), but more $U - B$ data are needed.

Spectra and light curves of SNe Ia also are correlated with the nature of the parent galaxies. On average, SNe Ia in red or early-type galaxies have lower values of $V_{10}(\text{Si})$ and faster light curves than those in late-type or blue galaxies (Hamuy et al 1995b, 1996a, Branch et al 1996b). The Δm_{15} parameter is plotted against the color of the parent galaxy in Figure 6.

Now we consider correlations with absolute magnitude, which are the ones that are needed for improving on the standard-candle approach to H_0 . Using Tully-Fisher (TF) and surface-brightness-fluctuation (SBF) distances for a sample of nine SNe Ia, including the peculiar SNe 1991T, 1986G, and 1991bg and the not-so-well-observed SN 1971I, Phillips (1993) found correlations between absolute magnitude (M_B , M_V , and M_I) and Δm_{15} . At one extreme SN 1991T was overluminous and somewhat slow to decline, and at the other SN 1991bg was extremely subluminous and quick to decline. The correlation was in the same sense as that proposed by Pskovskii (1977). Subsequently, the Calán-Tololo data on SNe Ia in the Hubble flow, for which the relative distances are more secure, showed that the correlation indicates considerable scatter among the dim, red, rapidly-declining events. After adopting a color cut to eliminate the three observationally red events in their sample, Hamuy et al (1996b) derived slopes $dM_B/d\Delta m_{15} = 0.78 \pm 0.17$, $dM_V/d\Delta m_{15} = 0.71 \pm 0.14$, and $dM_I/d\Delta m_{15} = 0.58 \pm 0.13$ (Figure 7). These slopes are much less steep than those that were obtained by Phillips (1993), yet definitely greater than zero. The Hubble diagram in V for the 26 non-red events, standardized by means of Δm_{15} , is shown in the *bottom panel* of Figure 4. When the correlations with Δm_{15} were taken into account, the absolute-magnitude dispersions fell

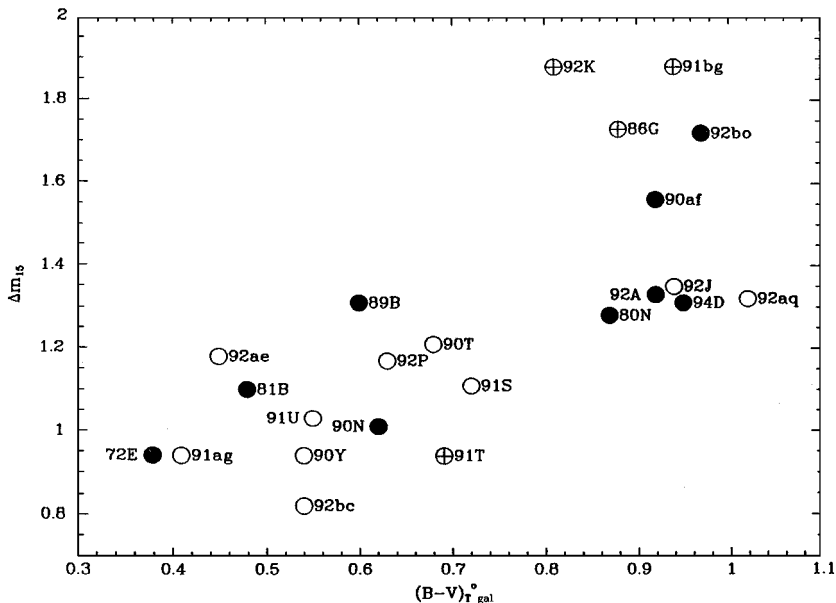


Figure 6 Light-curve decline rate Δm_{15} is plotted against parent galaxy color, corrected to face-on inclination. From Branch et al (1996b).

from those quoted in Section 2.1.3 to $\sigma_{\text{obs}}(M_B) = 0.17$, $\sigma_{\text{obs}}(M_V) = 0.14$, and $\sigma_{\text{obs}}(M_I) = 0.13$. Tripp (1997) found slopes that agreed well with those of Hamuy et al (1996b). In a straightforward but rigorous statistical analysis of the Calán-Tololo data, Tripp (1998) also introduced a linear dependence of absolute magnitude on $B - V$ and found that $dM_B/d\Delta m_{15}$ falls to about 0.5; that $B - V$ is more effective than Δm_{15} in standardizing absolute magnitudes; and that the two-parameter corrections transform the Calán-Tololo sample into perfectly standardized candles insofar as can be measured with current techniques.

Absolute magnitude also correlates with the spectroscopic indices discussed by Fisher et al (1995) and Nugent et al (1995c), with parent-galaxy type (Hamuy et al 1996a, Saha et al 1997), and with parent-galaxy color (Hamuy et al 1995b, Branch et al 1996b). On average, normal SNe Ia in early-type or red galaxies appear to be dimmer by 0.2 or 0.3 mag than those in late-type or blue galaxies, and the absolute-magnitude dispersions of non-red SNe Ia in blue and in red galaxies, considered separately, are only about 0.2.

In an analysis that bears on many of the issues that have been discussed in this section, Riess et al (1995a, 1996a) have developed a formal statistical

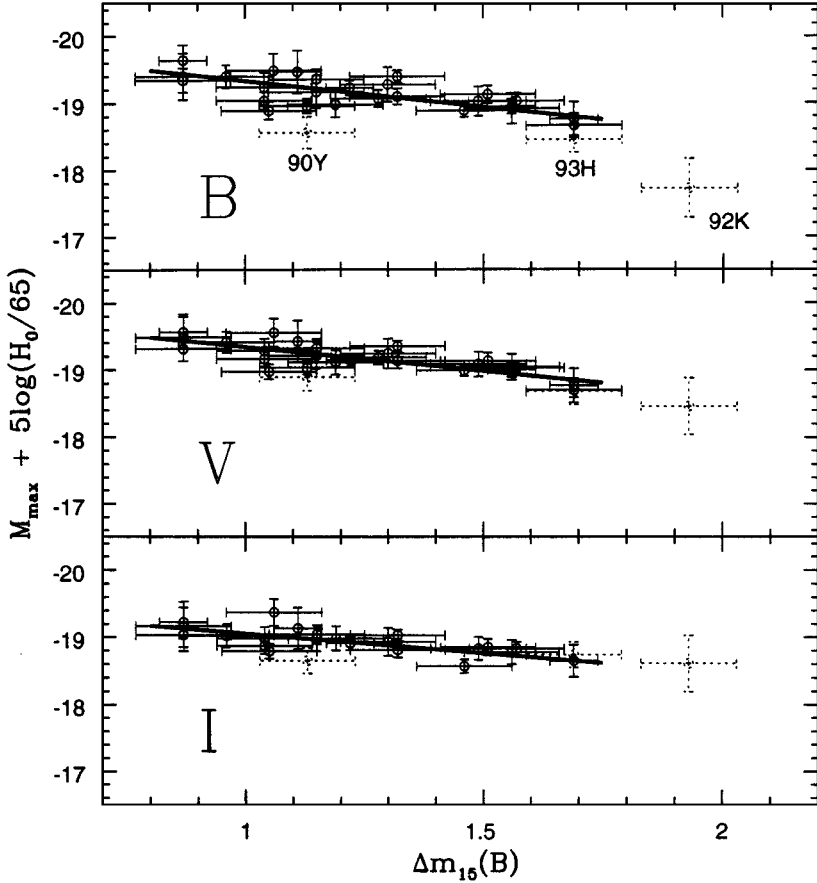


Figure 7 Absolute magnitudes of the Calán-Tololo SNe Ia are plotted against light-curve decline parameter Δm_{15} , with weighted linear least-square fits that exclude the observationally red SNe 1990Y, 1993H, and 1993K. From Hamuy et al (1996a).

procedure to simultaneously estimate extinctions, relative luminosities, and relative distances from the shapes of light curves in the B , V , R , and I bands (multicolor light-curve shapes: MLCS). A training set of 9 SNe Ia with adopted distance and extinction estimates was used to establish a linear relationship between luminosities and light-curve shapes. Then individual extinctions, relative luminosities, and relative distances were inferred for an independent set of 20 Hubble-flow SNe Ia (including 10 from the Calán-Tololo survey) from their light curves. An attractive feature of MLCS is that it yields formal error

estimates. The analysis gave results for various SN Ia properties such as relations between $B - V$, $V - R$, and $R - I$ color curves and luminosity (Figure 8), and the dispersion in the MLCS distance moduli was found to be only 0.12 mag. These SN Ia properties are less directly “observational” than those discussed earlier in this section because they depend on the adopted properties of the training set, including TF and SBF relative distances, and on an assumed a priori probability distribution of the extinction. Of the 9 training-set events, 8 also were in the sample of 9 that was used by Phillips (1993) to derive magnitude-decline slopes that proved to be too steep, and the maximum-light $B - V$ as parameterized by Riess et al (1996a) correlates with luminosity (Lira 1996) and Δm_{15} (R Tripp, private communication) in ways that the Hubble-flow events of the Calán-Tololo sample do not. Assessing the consequences of changing the MLCS input data is not trivial; it will be interesting to see whether and how the results of MLCS change when the nearby training set is replaced by a subset of the Hubble-flow SNe Ia, whose relative distances will be more secure. See Riess et al (1998) for an interesting proposal to circumvent the labor of obtaining accurate multicolor light-curve shapes by combining the information carried in a single spectrum and a single-epoch measurement of B and V magnitudes to determine “snapshot” distances to SNe Ia.

2.3 Summary

SNe Ia can be divided into a majority of “normal” events that have highly homogeneous properties and a minority that are “peculiar.” When normals and peculiars are considered together, correlations among their observational properties are obvious. To a certain extent, the correlations hold among normal SNe Ia, and the concept of a sequence of SNe Ia ranging from those having high-excitation spectra, high blueshifts of spectral features, slow light curves, and high luminosities to those having low-excitation spectra, low blueshifts, fast light curves, and low luminosities is useful. The former tend to occur in blue, late-type galaxies and the latter in red, early-type galaxies. A one-dimensional sequence of SNe Ia is not, however, the whole story.

A simple $B - V$ cut that eliminates events that are observationally red at maximum light yields a sample of nearly standard candles having $\sigma_{\text{obs}}(M_B) \simeq \sigma(M_V)_{\text{obs}}$ less than 0.3. Correlations between absolute magnitude and one or more SN Ia or parent-galaxy observables can be used to further standardize the absolute magnitudes to better than 0.2 mag. As far as determining the value of H_0 by means of Cepheid-calibrated SNe Ia is concerned, the accuracy of the result will depend not only on the tightness of the intrinsic correlation among normal SNe Ia but also on the degree to which the relevant distance-independent observables happen to be known for the Cepheid-calibrated SNe Ia.

3. H_0 FROM CEPHEID CALIBRATIONS

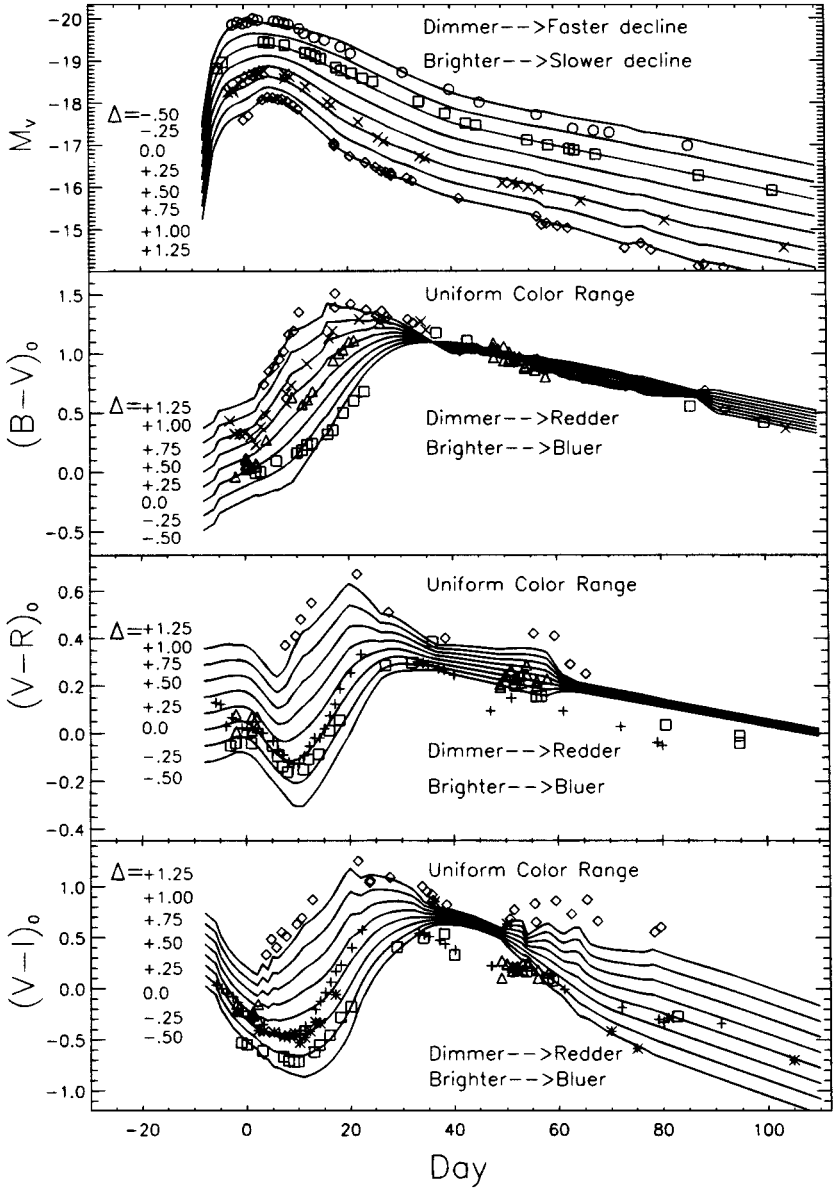
Cepheid-based calibrations of the absolute magnitudes of SNe Ia began with the discovery and measurement of Cepheid variables in IC 4182, the parent galaxy of SN 1937C, by the HST SN Ia Consortium (Sandage et al 1992, Saha et al 1994). The Cepheid distance modulus of IC 4182, $\mu = 28.36 \pm 0.09$, proved to be in agreement with the modulus that had been obtained much earlier by Sandage & Tammann (1982) on the basis of the brightest red stars in IC 4182, $\mu = 28.21 \pm 0.2$. As of this writing, the Consortium has determined Cepheid distances to four other galaxies in which five SNe Ia have appeared and hopes to be able to determine the distances to at least three more galaxies, including NGC 3627, the parent of SN 1989B; NGC 4527, the parent of SN 1991T; and NGC 1316 \equiv Fornax A, the rather early-type (Sa peculiar) parent of SNe 1980N and 1981D. The HST H_0 Key Project team (Freedman et al 1997) is expected to contribute a distance to NGC 4414, the parent of SN 1974G.

A critical assessment of the reliability of the Cepheid distances is beyond the scope of this article. Thorough discussions of the discovery and photometry of the Cepheids, the observed period-luminosity relations, and the extinction and derived distances are given in the papers of Saha et al (1994, 1995, 1996a,b, 1997). The Consortium uses the V and I band Cepheid period-luminosity ($P-L$) relations of Madore & Freedman (1991), which are assumed to be independent of metallicity. Mild revision of the zero-points of the $P-L$ relations on the basis of parallaxes of Galactic Cepheids measured by the *Hipparcos* satellite, in the sense of making Cepheid distances longer and Cepheid-based estimates of H_0 lower, may prove to be required (Feast & Catchpole 1997, Sandage & Tammann 1998, Madore & Freedman 1998) at the level of 4%. The metallicity dependence of Cepheid distances (Gould 1994, Kochanek 1997, Saha et al 1997, Sasselov et al 1997, Kennicutt et al 1998) is an important issue, but the $P-L$ relations in M_{bol} appear to be independent of $[\text{Fe}/\text{H}]$ at the level of 0.05 mag for even a change of 1.7 dex in the metallicity (Stothers 1988, Choisi et al 1992, Sandage 1996, Saio & Gautschi 1998).

3.1 *The Cepheid-Calibrated SNe Ia*

Table 6 of Saha et al (1997) lists distance moduli, apparent magnitudes, and absolute magnitudes for seven Cepheid-calibrated SNe Ia: SN 1937C in IC

Figure 8 An empirical family of SN Ia light and color curves parameterized by luminosity. Data for some training-set members are shown as *open circles* (SN 1991T), *open squares* (1994ae), *triangles* (1980N), *plus signs* (SN 1992A), *crosses* (1986G), and *open diamonds* (1991bg). The *lines* are the light and color curves constructed from the training-set data, parameterized in terms of relative absolute magnitude (Δ). From Riess et al (1996a).



4182, SNe 1895B and 1972E in NGC 5253, SN 1981B in NGC 4536, SN 1960F in NGC 4496A, SN 1990N in NGC 4639, and SN 1989B in NGC 3627. The Cepheid distance of the last galaxy has not yet been determined directly; it is assigned the mean Cepheid distance of three fellow members of the Leo group of galaxies. There has been little disagreement about the apparent magnitudes of these calibrator SNe Ia except in the case of SN 1937C (Schaefer 1994, 1996a, Pierce & Jacoby 1995, Jacoby & Pierce 1996). Extinction of the calibrators by dust in our Galaxy is low. Estimates of the extinction of the SNe Ia by dust in the parent galaxies are not so easy to come by, but parent-galaxy extinction of at least four of the calibrators, SNe 1895B, 1937C, 1960F, and 1972E, is likely to have been quite low. Saha et al (1997) assumed that the total extinction of these four was the same as the (low) mean extinction of the corresponding Cepheids, in which case the apparent distance modulus of the Cepheids combined with the apparent magnitude of the SN Ia gives the extinction-free SN Ia absolute magnitude. For SNe 1981B, 1989B, and 1990N, Saha et al (1997) obtained absolute magnitudes using the extinction-corrected distance moduli of the Cepheids together with assumed SN extinctions of $E(B - V) = 0.1, 0.37$ (Wells et al 1994), and 0.00, respectively. The mean absolute magnitudes listed by Saha et al (1997) are $M_B = -19.52 \pm 0.07$ based on seven events and $M_V = -19.48 \pm 0.07$ based on six events.

Spectroscopically, SNe 1960F, 1981B, 1989B, and 1990N were observed at maximum light and they were normal. The earliest spectra of SNe 1937C and 1972E were obtained long enough after maximum light to raise the issue of whether they could have been peculiar in the sense of SN 1991T; arguments that they were spectroscopically normal have been made by Branch et al (1993, 1994). The single spectrum of SN 1895B (Schaefer 1995a) is consistent with normal, but an SN 1991T-type peculiarity cannot be excluded.

The inclusion of SN 1895B as a calibrator has been questioned on the grounds that its apparent magnitude may be unreliable, but Saha et al (1995) argued that it would be arbitrary to exclude it because there is no reason to expect a *systematic* error in its apparent magnitude. Also, it must be remembered that the uncertainty in a calibrator's absolute magnitude depends on the uncertainties not only in the apparent magnitude but also in the extinction and in the distance modulus; thus the uncertainties in the absolute magnitudes of the calibrators listed by Saha et al (1997) turn out to be of comparable size. The possibility that SN 1895B was a peculiar event like SN 1991T may be a better argument for its exclusion. If it is excluded, and if the most recent (and fainter) estimates of the apparent magnitudes of SN 1937C (Jacoby & Pierce 1996) and SN 1990N (Lira et al 1998) are adopted, the mean absolute magnitudes of the seven calibrators only drop from the values of Saha et al (1997), $M_B = -19.52$ and $M_V = -19.48$, to $M_B = M_V = -19.44$.

In principle, the calibrators could provide an independent test of the magnitude-decline relation found for the Hubble-flow SNe Ia, but considering the uncertainties in the absolute magnitudes and the decline rates of the calibrators, the shallow slopes found by Tammann & Sandage (1995) and Hamuy et al (1996a) can be neither confirmed nor denied. It is worth noting, though, that invoking a strong metallicity dependence of the Cepheid zero point, in the sense of reducing the Cepheid distances to metal-deficient galaxies (IC 4182, NGC 5253) relative to the distances of more metal-rich galaxies, would lead to an *inverse* magnitude-decline relation that is not plausible. This is a reason to doubt that introducing a metallicity dependence will cause any substantial revision of the results discussed in the next section.

3.2 *Matching the Calibrators to the Hubble Flow*

The ways that have been used to obtain H_0 by comparing the local Cepheid-calibrated SNe Ia to Hubble-flow SNe Ia are considered here more or less in order of increasing complexity.

The intent of the HST SN Ia Consortium all along has been to simply treat SNe Ia as nearly standard candles. In their most recent paper, Saha et al (1997) assigned mean values for M_B and M_V of the calibrators to the mean values of 56 non-red ($B - V < 0.2$) Hubble-flow SN Ia to obtain $H_0 = 58_{-8}^{+7}$, where extinction of the non-red Hubble-flow SN Ia is neglected. Saha et al emphasized that for H_0 higher than 65, nearly all of the Hubble-flow SNe Ia would be intrinsically dimmer than nearly all of the Cepheid-calibrated SNe Ia (Figure 9), in spite of the observational bias in favor of discovering the most luminous of the Hubble-flow SNe Ia. The larger the SN Ia absolute-magnitude dispersion actually is (cf van den Bergh 1996), the stronger an argument this is for a low value of H_0 because the effect of the bias increases with the size of the dispersion. For an insightful discussion of the effects of selection bias on distance determinations, see Teerikorpi (1997) in this series.

Others have used Saha et al's Cepheid distances, together with slightly different adopted apparent magnitudes of the SN Ia calibrators and in some cases using only subsets of the calibrators, to make their own estimates of H_0 . For example, the local calibrators are in blue galaxies, and since SNe Ia in blue galaxies tend to be more luminous than those in red galaxies, it would seem to be appropriate to match the calibrators only to Hubble-flow SNe Ia in blue galaxies. Branch et al (1996b) obtained $H_0 = 57 \pm 4$ in this way, and Saha et al (1997) showed that this hardly affects their result for H_0 . If a Cepheid distance to NGC 1316 can be obtained, it will provide a valuable calibration of two SNe Ia in an early-type red galaxy.

Another way to match the calibrators to Hubble-flow SNe Ia is to use the supernova $B - V$ color to standardize the absolute magnitudes. The correlation

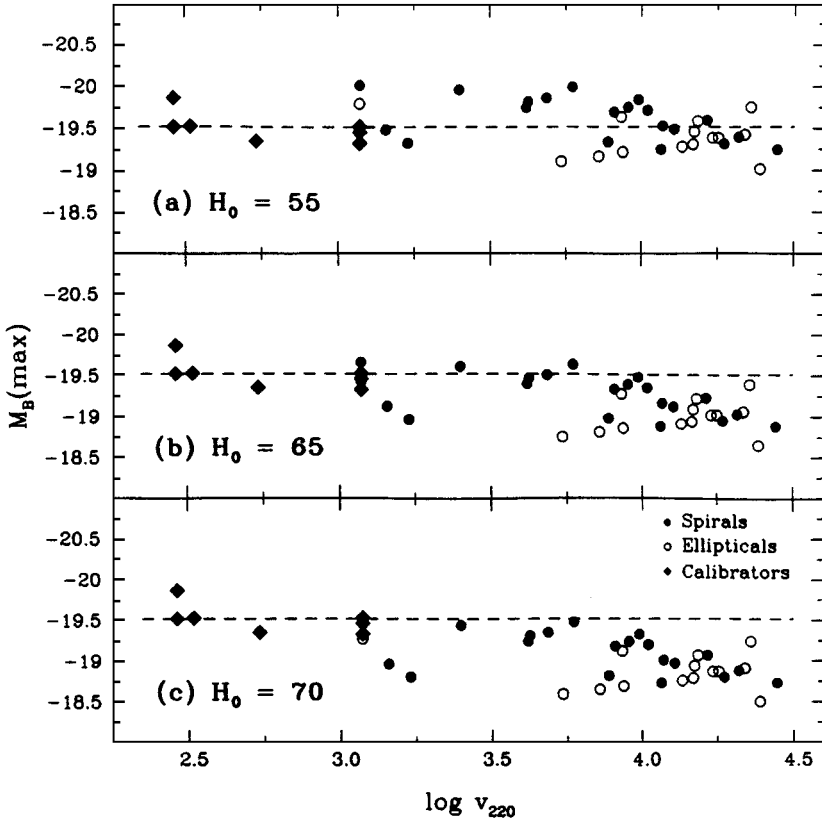


Figure 9 Absolute magnitude is plotted against distance modulus for Cepheid-calibrated SNe Ia (diamonds) and other non-red SNe Ia after 1985 (circles). The absolute magnitudes of the latter are shown for three values of H_0 . From Saha et al (1997).

between absolute magnitude and $B - V$ will be anything but perfect because even if a one-to-one intrinsic relation existed, it wouldn't be exactly like the relation produced by extinction. Nevertheless this approach has the attractive feature that it requires no extinction estimates for the calibrators *or* the Hubble-flow events. In this way, Branch et al (1996a), using several subsets of calibrators (none of which included SN 1895B because there is no estimate of its V magnitude) and several subsets of Hubble-flow SNe Ia, obtained values of H_0 ranging from 54 ± 5 to 60 ± 6 .

The standardization method for absolute magnitudes that has received the most attention so far is the use of light-curve decline rates or shapes. Hamuy

et al (1996b) matched the calibrators to their non-red Hubble-flow SNe Ia using their linear relations between absolute magnitude and Δm_{15} and obtained $H_0 = 63 \pm 3.4$ (internal) ± 2.9 (external). The requirement of an accurate value of Δm_{15} restricted the number of calibrators to four: SNe 1937C, 1972E, 1981B, and 1990N; extinction of the non-red Hubble-flow SNe Ia was neglected. Schaefer (1996b) considered the apparent magnitudes of the calibrators in the U , B , V , and H bands (where possible) and obtained $H_0 = 55 \pm 3$. Kim et al (1997) matched the calibrators to five of Perlmutter et al's (1997c) high-redshift SNe Ia with the two samples adjusted to a common mean value of Δm_{15} and obtained estimates of H_0 that depend slightly on the values of Ω_m and Ω_Λ (see their figure 3). For example, for $\Omega_m = 1$ and $\Omega_\Lambda = 0$, their result for H_0 was 59 ± 3 , whereas for $\Omega_m = 0.3$ and $\Omega_\Lambda = 0$, it was 62 ± 4 . Tripp (1997) matched the calibrators to a combination of the Calán-Tololo and high-redshift samples, all adjusted to a common mean Δm_{15} , and obtained $H_0 = 60 \pm 5$. When Tripp (1998) allowed absolute magnitude to depend linearly on both $B - V$ and Δm_{15} , he obtained $H_0 = 60 \pm 6$. Freedman et al (1997) assumed that a Cepheid-based distance to the spiral galaxy NGC 1365 gives the distance to the Fornax cluster and to the early-type galaxies NGC 1380, the parent of SN 1992A, and NGC 1316, the parent of SN 1980N; by applying a magnitude-decline relation to these two events together with some of the other calibrators, they obtained $H_0 = 67 \pm 8$. But assigning the distance of NGC 1365 to the early-type parent galaxies of SNe 1992A and 1980N is highly controversial (Freedman 1997, Saha et al 1997, Sandage & Tammann 1997, Tammann & Federspiel 1997).

Riess et al (1996a) used their MLCS technique with three calibrators, SNe 1972E, 1981B, and 1990N, to calibrate the absolute distances to their sample of 20 Hubble-flow SNe Ia and obtained $H_0 = 64 \pm 3$ (statistical) ± 6 (total error). In this approach, individual extinctions of the Hubble-flow events are derived rather than assumed or neglected.

3.3 Summary

The mild differences between the results for H_0 quoted in this section are due to differences in the numbers of calibrators that are used and in the ways that they are matched to Hubble-flow SNe Ia. Different people would assign different relative weights to these analyses. In principle, the analyses that try to take diversity into account are preferred, but at present, some of these can use only a small number of calibrators. Suffice it to say that present Cepheid calibrations of SNe Ia give values of H_0 near 60. Mild revision is to be expected as more Cepheid-calibrated and Hubble-flow SNe Ia become available, as the zero-points of the Cepheid $P - L$ relations are revised, and as a Cepheid metallicity dependence is taken into account if needed.

4. PHYSICAL PROPERTIES

The immediate progenitors of SNe Ia are believed to be carbon-oxygen (C-O) white dwarfs in close binary systems, and no other kind of progenitor has been under serious consideration for some time. During the 1980s, general consensus was also that the first nuclear ignition was of carbon, deep inside the white dwarf. This event would be followed by the outwards propagation of a subsonic nuclear flame (a “deflagration”), the velocity of which had to be (and still has to be) parameterized. One particular nuclear-hydrodynamical deflagration model called W7 (Nomoto et al 1984) was parameterized in such a way that its radial composition structure with (Branch et al 1985) or without (Harkness 1991a) ad hoc compositional mixing of its outer layers was able to give a good account of the spectral features of normal SNe Ia. Thus W7 became the standard SN Ia model, and this is where matters stood when the physics of SNe was reviewed in this series by Woosley & Weaver (1986) and still at the time of Branch & Tammann (1992). Since then, many people have put much effort into seeking the nature of the progenitor binary systems, constructing hydrodynamical explosion models, and calculating light curves and spectra of models.

4.1 *Progenitors*

Although numerous articles and several recent reviews (Branch et al 1995, Renzini 1996, Iben 1997, Ruiz-Lapuente et al 1997a) have been written about SN Ia progenitors, we still do not know even whether (or how often) the progenitor binary system contains one white dwarf or two.

In the standard “single-degenerate” scenario, the white dwarf accretes from the Roche lobe or wind of a nondegenerate companion until it approaches the Chandrasekhar mass and ignites carbon deep in its interior. There has been much recent interest in the possibility that single-degenerate pre-SN Ia systems are being observed as supersoft X-ray sources (van den Heuvel et al 1992, Rappaport et al 1994, Yungelson et al 1996), especially since Hachisu et al (1996) found a new strong-wind solution for mass transfer from a lobe-filling companion. According to Hachisu et al, the formation and expulsion of a common envelope can be avoided more easily than previously believed. This may open up two promising channels (Figure 10) for the accretor to reach the Chandrasekhar mass, and both could be observed as supersofts: close systems in which the donor is a main sequence or subgiant star in the range $2\text{--}3.5 M_{\odot}$ and wide systems in which the donor is a red giant of $\simeq 1 M_{\odot}$ (Hachisu et al 1996, Nomoto et al 1997, Li & van den Heuvel 1997, but see Yungelson & Livio 1998). In the single-degenerate scenario, a significant amount of circumstellar matter is expected to be in the vicinity of the explosion. So far, no convincing evidence

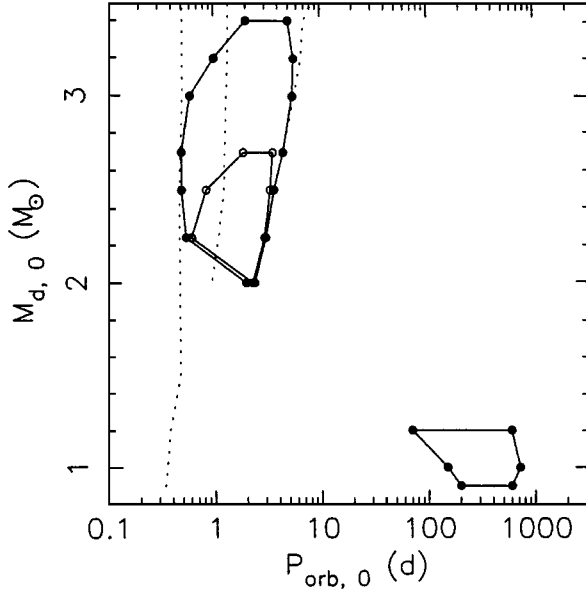


Figure 10 Donor masses are plotted against orbital period for candidate single-degenerate SN Ia progenitor binary systems. Filled circles are for an initial white-dwarf accretor of $1.2 M_{\odot}$ and open circles are for $1.0 M_{\odot}$. The dotted lines represent the boundaries of mass transfer in case A (left) and case B (right). From Li & van den Heuvel (1997).

for narrow circumstellar hydrogen or helium lines in SN Ia spectra has been found (Ho & Filippenko 1995, Cumming et al 1996), nor has X-ray (Schlegel & Petre 1993) or radio (Eck et al 1996) emission from circumstellar interaction been seen. These nondetections are not yet quite stringent enough, however, to rule out single-degenerate progenitor systems (Lundqvist & Cumming 1997). So far, only one SN Ia has been found to be polarized (Wang et al 1997b); the general lack of polarization may lead to constraints on the presence of circumstellar matter and the nature of the progenitor systems (Wang et al 1996).

In the standard “double-degenerate” scenario, two white dwarfs spiral together as a consequence of the emission of gravitational radiation to form a super-Chandrasekhar merger product. According to a population-synthesis study by Tutukov & Yungelson (1994), mergers that form within 3×10^8 years of star formation have a mean mass that is greater than $2 M_{\odot}$ (Figure 11). Those researchers who have made recent attempts to model the merging process using SPH calculations (Mochkovitch & Livio 1990, Benz et al 1990, Rasio & Shapiro 1995, Mochkovitch et al 1997) are not uniformly optimistic about producing

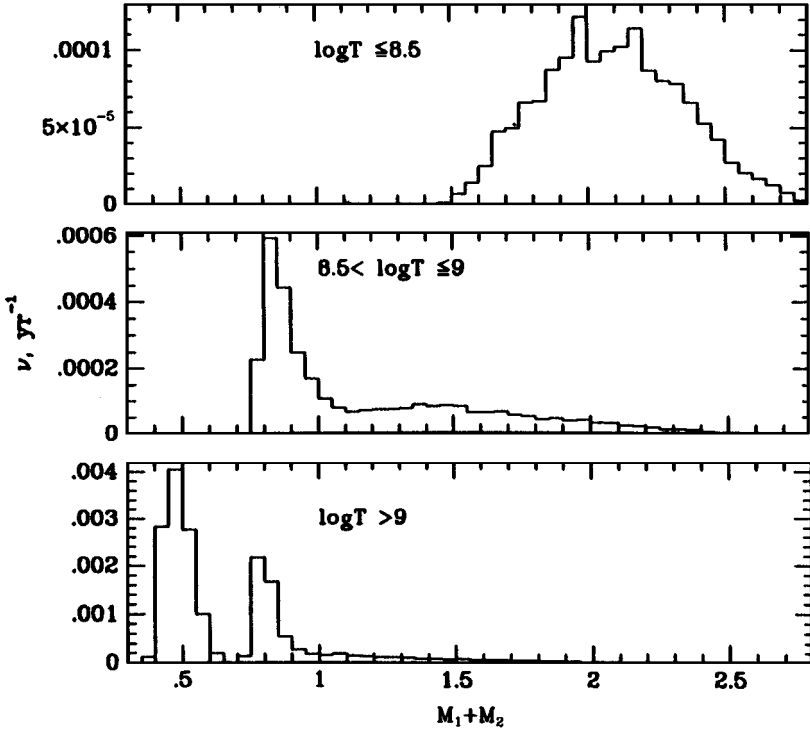


Figure 11 The distributions of the masses of double-degenerate mergers for three age intervals. The peaks near 2.0, 0.8, and 0.5 M_{\odot} correspond to CO-CO, CO-He, and He-He white-dwarf mergers. Explosions are not expected for total masses below 1.4 M_{\odot} . From Tutukov & Yungelson (1994).

SNe Ia in this way. On the other hand there are arguments (Section 4.4) that peculiar events like SN 1991T, at least, may be super-Chandrasekhar merger products. It is not clear that there should be a significant amount of circumstellar matter in the vicinity of a merger SN Ia, but if so, it would be carbon and oxygen rather than hydrogen and helium. In this regard, the detection of narrow [O I] lines in late-time spectra of SN 1937C by Minkowski (1939) and the possible detection of narrow [O I] $\lambda 8446$ emission in a very early spectrum of SN 1991T by Ruiz-Lapuente et al (1992) are intriguing.

4.2 Explosion Models

In the 1990s, a variety of explosion models other than the classical deflagration has been considered. They can be divided into “carbon ignitors” and “helium

ignitors” according to whether the first nuclear ignition is of carbon, deep inside the accretor, or of helium near the surface.

Among the carbon-ignitor models, deflagrations, “delayed detonations” (Khokhlov et al 1993, Arnett & Livne 1994a,b, Woosley & Weaver 1994b, Höflich 1995, Nomoto et al 1997), and “pulsating delayed detonations” (Khokhlov et al 1993) could be applicable in the single-degenerate case, so these have been constructed for Chandrasekhar-mass ejection. In the double-degenerate case, the classical idea (see Iben 1997 for a review) is that the merger leads to a super-Chandrasekhar configuration consisting of a white-dwarf core, a quasispherical pressure-supported envelope, and a low-density thick disk. Whether this flying saucer (Iben & Tutukov 1984) eventually explodes or collapses is thought to depend on, among other things, whether carbon ignites at the core-disk boundary and burns steadily inward to produce an oxygen-neon-magnesium configuration that will simply collapse to a neutron star. A different possibility is that explosion of one and then the other white dwarf occurs during or even just before the merger, owing to tidal or shear heating (Iben 1997). Shigayama et al (1992) and Khokhlov et al (1993) constructed some spherically symmetric explosion models with super-Chandrasekhar merger products in mind.

In the 1990s, there has been much interest in sub-Chandrasekhar helium-ignitor models, as constructed by Woosley & Weaver (1994a), Livne & Arnett (1995), and Höflich & Khokhlov (1996). The first nuclear ignition is near the bottom of a helium layer of about $0.2 M_{\odot}$ accumulated on top of a C-O white dwarf. A prompt detonation propagates outwards through the helium while an inward nonburning pressure wave compresses and ignites the underlying C-O (perhaps well off center) and drives a second detonation outwards through the C-O. Owing to the difference between the nuclear kinetics of carbon and helium burning, these models have a composition structure that is fundamentally different from that of carbon ignitors. ${}^4\text{He}$ burns to ${}^{12}\text{C}$ by the slow triple alpha process, and as soon as ${}^{12}\text{C}$ is formed, it rapidly captures alpha particles to form ${}^{56}\text{Ni}$, so the original helium layer ends up as a high-velocity mixture of ${}^{56}\text{Ni}$ and leftover ${}^4\text{He}$. In these models intermediate-mass elements such as silicon and sulfur, produced by low-density carbon burning, are ejected in a relatively narrow range of velocity around $10,000 \text{ km s}^{-1}$.

4.3 *Light Curves*

Harkness (1991b) first carried out light-curve calculations that took into account the dependence of the opacity on temperature, density, and composition, and he found that the light curve of model W7 was about right for normal SNE Ia. Machinery developed for calculating gamma-ray deposition (Höflich et al 1992) and bolometric and monochromatic light curves (Höflich et al 1993) led

to a major computational effort by Höflich & Khokhlov (1996), who calculated local thermodynamic equilibrium (LTE) light curves for 37 explosion models encompassing each of the kinds mentioned above. The light curves and colors of Chandrasekhar-mass carbon-ignitor models depend mainly on the amount of ^{56}Ni that is ejected: Models with more ^{56}Ni are hotter and brighter, and, because the opacity increases with temperature in the range of interest, they have broader light curves. Carbon-ignitor models can account reasonably well for the photometric properties of both normal and peculiar weak SNe Ia (Wheeler et al 1995, Höflich et al 1996, 1997), with normal SNe Ia requiring $M_{\text{Ni}} \simeq 0.6 M_{\odot}$ (Figure 12) and SN 1991bg requiring only about $0.1 M_{\odot}$. The differences between the calculated light curves for different kinds of carbon-ignitor models that eject similar amounts of ^{56}Ni are fairly subtle, so deciding just which kind of explosion model applies to any particular SN Ia on the basis of its light curves and colors alone is difficult.

Discriminating between carbon ignitors and helium ignitors is more straightforward because they have such different compositions. Höflich & Khokhlov (1996) found their helium-ignitor models to be inferior to the carbon ignitors

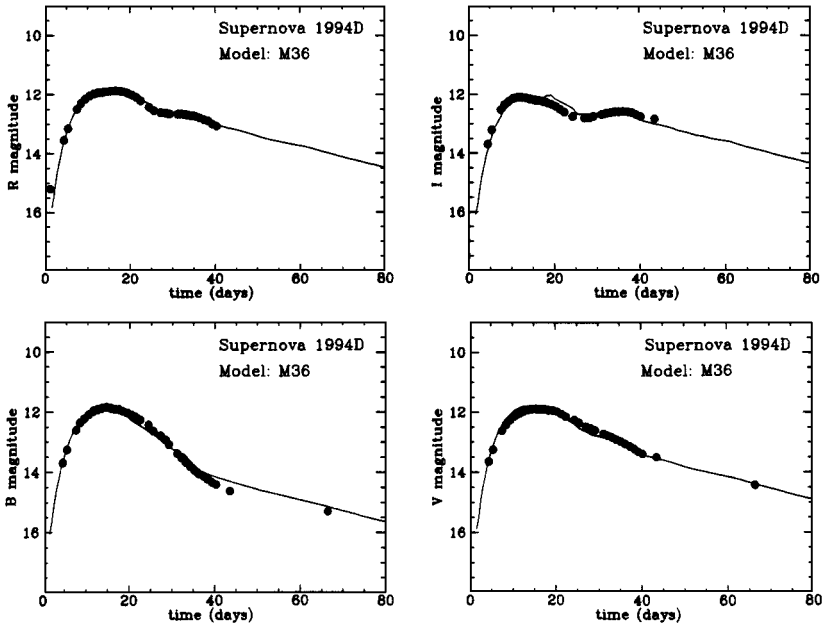


Figure 12 Observed light curves of SN 1994D are compared with calculated light curves for model M36, a delayed detonation that ejected $M_{\text{Ni}} = 0.6 M_{\odot}$ and reached $M_V = -19.4$. From Höflich (1995).

in producing the light curve and colors of a normal bright SN Ia. The helium ignitors do not work at all for subluminous SN Ia like SN 1991bg because the ^{56}Ni in the outer layers keeps the photosphere hot and the colors too blue.

4.4 Spectra

Synthetic spectrum calculations that assumed LTE but were otherwise detailed and self-consistent were carried out by Harkness (1991a,b). He found that the spectra of model W7 closely resembled those of the normal SNE Ia 1981B (Figure 13) and concluded that the ejected ^{56}Ni mass needs to be in the range

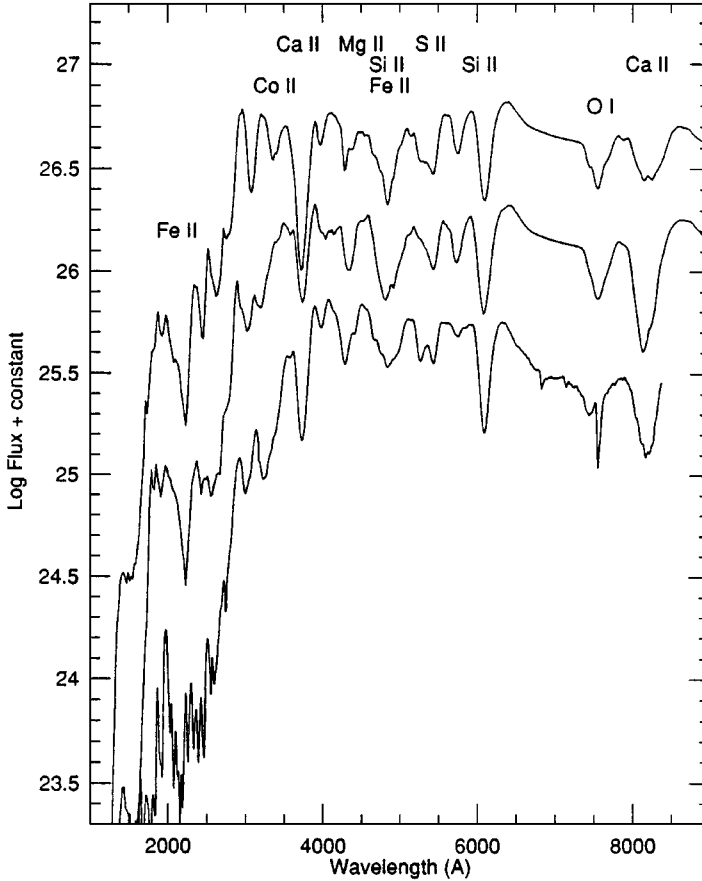


Figure 13 Local thermodynamic equilibrium (LTE) spectra calculated for model W7, 14 days after explosion, with no mixing (*top*) and mixing for $v > 11,000 \text{ km s}^{-1}$ (*center*), are compared with the maximum-light spectrum of SN 1981B (*bottom*). From Harkness (1991a).

0.5–0.8 M_{\odot} , with the W7 value, 0.6 M_{\odot} , appearing to be optimum. Recently, detailed nonlocal thermodynamic equilibrium (NLTE) spectrum calculations have begun to be made (e.g. Baron et al 1996, Pauldrach et al 1996). Höflich (1995) compared synthetic spectra of delayed-detonation models with spectra of SN 1994D and found that models having $M_{\text{Ni}} \simeq 0.6$ provided the best fits. Nugent et al (1995a, 1997) found that W7 models provided good fits to the spectra of SNe 1981B, 1992A, and 1994D (Figure 14). Nugent et al (1995c) adopted the W7 composition structure and varied just the effective temperature

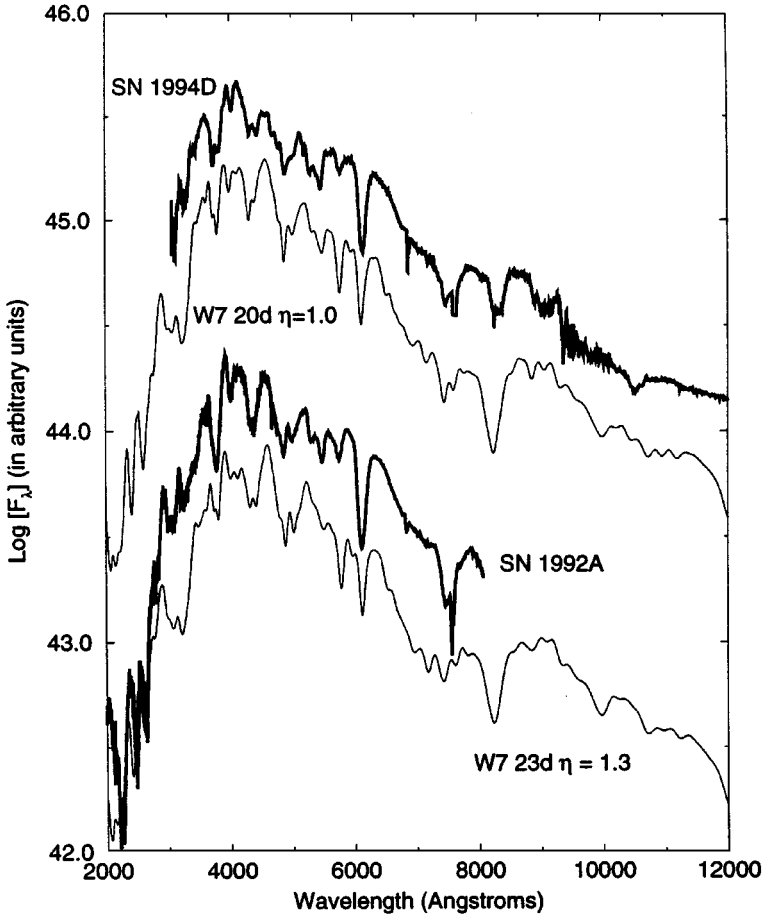


Figure 14 NLTE spectra calculated for model W7 are compared to spectra of SN 1994D at maximum light and SN 1992A 5 days after maximum light. From Nugent et al (1997).

to generate a sequence of maximum-light spectra that resembled the sequence of observed maximum-light spectra all the way from SN 1991bg through SN 1986G and normal SN Ia to SN 1991T (Figure 1, *left panel*). This means that the differences between the maximum-light spectra of SNe Ia, like the differences between the spectra of stars, are mainly due to differences in temperature. The root cause of the temperature range in real SNe Ia presumably is a range in M_{Ni} , and the whole composition structure surely also varies along the sequence in a way that has yet to be determined.

Höflich et al (1997) and Nugent et al (1997) also calculated spectra of helium-ignitor models and found that they did not give satisfactory fits to the spectra of SNe Ia. The exploration of helium-ignitor models was well motivated on physical grounds (Livne 1990, Woosley & Weaver 1994a), so the interesting question about them is why do we not see them? It should be acknowledged here that on the basis of their calculations of late nebular spectra of explosion models, Liu et al (1997a,b) favored sub-Chandrasekhar mass ejection for normal SNe Ia and even SN 1991T; Ruiz-Lapuente (1996) did not. The calculation of nebular spectra is hampered by a lack of reliable atomic data, although the situation is improving (Liu et al 1997c). In any case, it is not clear why sub-Chandrasekhar C-O white dwarfs that lack the deadly surface helium layer of the helium-ignitor models should explode. Another issue with respect to the nebular phase is that there are indications from light-curve shapes (Cappellaro et al 1998, Colgate et al 1997, Milne et al 1998) that at late times, positrons from Co^{56} decay are not completely trapped, as is usually assumed.

Detailed NLTE spectrum calculations are invaluable for falsifying hydrodynamical models, but since the number of parameterized hydro models that can be imagined is infinite and the number of spectra that can be calculated in NLTE is limited by computational complexity, a much more empirical approach to SN spectroscopy also is useful. Fisher et al (1997) used a fast, parameterized spectrum synthesis code to study a high-quality spectrum of the normal SN Ia 1990N that was obtained 14 days before maximum light by Leibundgut et al (1991a). Fisher et al (1997) suggested that the absorption observed near 6040 Å, which had been attributed to $\lambda 6355$ of Si II, actually was produced by $\lambda 6580$ of C II in a high-velocity ($v > 26,000 \text{ km s}^{-1}$) carbon-rich region. Such a layer would be consistent with published delayed-detonation models. A Fisher, D Branch, K Hatano, and E Baron (manuscript in preparation) suggest that in the peculiar SN 1991T, the “Si II” absorption is dominated by C II $\lambda 6580$ before and perhaps even at maximum light. On the basis of the empirical constraints on the composition structure of SN 1991T together with estimates of the luminosity of SN 1991T, which must be checked with a Cepheid distance, Branch (1998) and Fisher et al (manuscript in preparation, noted above) suggest that peculiar events like SN 1991T are superluminous, usually extinguished, substantially

super-Chandrasekhar mergers from the youngest populations that are able to produce SNe Ia in this way, $\sim 10^8$ years (Tutukov & Yungelson 1994).

4.5 Summary

SNe Ia appear to be carbon ignitors. If normal SNe Ia are Chandrasekhar-mass explosions in single-degenerate progenitor systems, their light curves and spectra indicate that they eject $M_{\text{Ni}} \simeq 0.6 M_{\odot}$. If they are mergers of double degenerates, they should be at least mildly super-Chandrasekhar and then should eject somewhat more ^{56}Ni to achieve the temperature needed to account for their spectra.

5. H_0 FROM PHYSICAL CONSIDERATIONS

To first order, there is a natural SN Ia peak luminosity—the instantaneous radioactivity luminosity, i.e. the rate at which energy is released by ^{56}Ni and ^{56}Co decay at the time of maximum light (Arnett 1982, Arnett et al 1985, Branch 1992). With certain simplifying assumptions, the peak luminosity is predicted to be identical to the instantaneous radioactivity luminosity. The extent to which they differ, for a hydrodynamical explosion model, can be determined only by means of detailed light curve calculations that take into account the dependence of the opacity on the composition and the physical conditions. The state of the art is represented by the calculations of Höflich & Khokhlov (1996). The calculated peak luminosity of the models turns out to be proportional to M_{Ni} within uncertainties, and for models that can be considered to be in the running as representations of normal SNe Ia (carbon ignitors that take longer than 15 days to reach maximum light in the V band), the characteristic ratio of the peak luminosity to the radioactivity luminosity is about 1.2 (Branch et al 1997). The physical reason that the ratio exceeds unity in such models was explained by Khokhlov et al (1993) in terms of the dependence of the opacity on the temperature, which is falling around the time of maximum light.

Höflich & Khokhlov's (1996) light-curve calculations can be used to estimate H_0 in various ways. Höflich & Khokhlov (1996) themselves compared the observed light curves of 26 SNe Ia (9 in galaxies having radial velocities greater than 3000 km s^{-1}) to their calculated light curves in two or more broadbands, to determine the acceptable model(s), the extinction, and the distance for each event. From the distances and the parent-galaxy radial velocities, they obtained $H_0 = 67 \pm 9$. Like the empirical MLCS method, this approach has the attractive feature of deriving individual extinctions. But identifying the best model(s) for a SN while simultaneously extracting its extinction and distance, all from the shapes of its light curves, is a tall order. This requires not only accurate calculations but also accurate light curves, and the photometry of some of the

SNe Ia that were used by Höflich & Khokhlov (1996) has since been revised (Patat et al 1997). And because Höflich & Khokhlov’s (1996) models included many more underluminous than overluminous SNe (the former being of interest in connection with weak SN Ia like SN 1991bg) while the formal light-curve fitting technique has a finite “model resolution,” a bias towards deriving low luminosities and short distances for the observed SNe Ia is possible.

There are less ambitious but perhaps safer ways to use Höflich & Khokhlov’s (1996) models to estimate H_0 that involve an appeal to the homogeneity of normal SNe Ia and rely only on the epoch of maximum light when both the models and the data are at their best. The 10 Chandrasekhar-mass models having $0.49 \leq M_{\text{Ni}} \leq 0.67$ —i.e. those having M_{Ni} within the acceptable range for normal SNe Ia—have a mean $M_{\text{Ni}} = 0.58 M_{\odot}$ and a mean $M_V = -19.44$. Alternatively, the five models (W7, N32, M35, M36, PDD3) that Höflich & Khokhlov (1996) found to be most often acceptable for observed SNe Ia have a mean $M_{\text{Ni}} = 0.58$ and a mean $M_V = -19.50$. Using $M_V = -19.45 \pm 0.2$ in Equation 1 gives $H_0 = 56 \pm 5$, neglecting extinction of the non-red Hubble-flow SNe Ia.

Höflich & Khokhlov’s (1996) light-curve calculations were used in another way by van den Bergh (1995). Noting that the maximum light M_V and $B - V$ values of the models obey a relation that mimics that which would be produced by extinction (Figure 15), he matched the model relation between M_V and $B - V$ to the relation of the observed Hubble-flow SN Ia and obtained values of H_0 in the range of 55–60, depending on how the models were weighted. If helium-ignitor models had been excluded, the resulting H_0 would have been a bit lower because the models are underluminous for their $B - V$ colors. This procedure has the virtue of needing no estimates of extinction. The same result can be seen from figure 3 of Höflich et al (1996), who plotted M_V versus $B - V$ for Höflich & Khokhlov (1996) models and for the Calán-Tololo SNe Ia. For the assumed value of $H_0 = 65$, the relations between M_V and $B - V$ for the models and the observed SNe Ia are offset, and H_0 would need to be lowered to about 55 to bring them into agreement.

In their figure 2, Höflich et al (1996) also plot M_V versus a V -band light-curve decline parameter that is analogous to Δm_{15} , for the models and for the Calán-Tololo SNe Ia. Again with $H_0 = 65$, the models and the observed SNe Ia are offset, with H_0 needing to be lowered to about 55 to bring them into agreement.

Distances to SNe Ia also can be derived by fitting detailed NLTE synthetic spectra to observed spectra. Nugent et al (1995b) used the fact that the peak luminosities inferred from radioactivity-powered light curves and from spectrum fitting depend on the rise time in opposite ways, in order to simultaneously derive the characteristic rise time and luminosity of normal SNe Ia and obtained $H_0 = 60_{-11}^{+14}$. If SN Ia atmospheres were not powered by a time-dependent

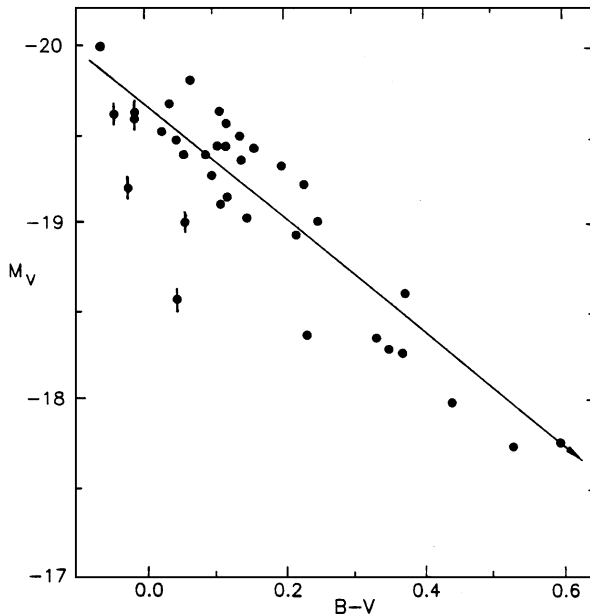


Figure 15 M_V is plotted against $B - V$ for the models of Höflich & Khokhlov (1996). Helium-ignitor models are indicated by vertical lines. The arrow has the conventional extinction slope of 3.1. Adapted from van den Bergh (1996).

energy source, the spectrum-fitting technique could be independent of hydrodynamical models. The procedure would be to look for a model atmosphere that accounts for the observed spectra without worrying about how that atmosphere was produced, estimate (or derive by fitting two or more phases) the time since explosion, and obtain the luminosity of the model. But, owing to the time-dependent nature of the deposition of radioactivity energy, SNe Ia “remember” their history (Eastman 1997, Nugent et al 1997, Pinto 1997). Light-curve and spectrum calculations really are coupled, and more elaborate physical modeling needs to be done.

6. CONCLUSION

The mean absolute magnitudes of the SNe Ia that have been calibrated by Cepheids in their parent galaxies are $M_B \simeq M_V \simeq -19.4$ or -19.5 . The same mean absolute magnitudes are calculated for explosion models that give a good account of SN Ia light curves and spectra, i.e. Chandrasekhar-mass

carbon-ignitor models that eject about $0.6 M_{\odot}$ of ^{56}Ni . Using $M_B = -19.45 \pm 0.2$ in Equation 1, based on the 26 non-red Calán-Tololo Hubble-flow events, would give $H_0 = 56 \pm 5$, but various workers using the Cepheid-based SN Ia absolute magnitudes and physical models in various ways have obtained values of H_0 ranging from about 54 to 67. Those who want a consensus value from SNe Ia with conservative errors could use, for now, $H_0 = 60 \pm 10$.

This value depends heavily on three things: the Cepheid distances of the HST SN Ia Consortium, the light-curve calculations of Höflich & Khokhlov (1996), and the observed light curves of the Calán-Tololo Hubble-flow SNe Ia. At present, the main issue about the Cepheid distances appears to be the possibility of a significant metallicity dependence. Some technical issues that bear on the accuracy of the complex light-curve calculations remain to be resolved, but the main issue here is the value of the ejected nickel mass, which in turn depends on whether the total ejected mass is Chandrasekhar, super-Chandrasekhar, or sub-Chandrasekhar. The main issue about the Hubble-flow SNe Ia probably has to do with selection bias. For example, many of the Calán-Tololo events peaked not far above the detection limit. If the Calán-Tololo events are selected from the bright end of the non-red SN Ia absolute-magnitude distribution, then the absolute-magnitude dispersions from the Calán-Tololo survey are probably too low, the mean absolute magnitude of non-red SNe Ia in Equation 1 is too bright (for a fixed H_0), and most of our current estimates of H_0 from SNe Ia probably are too high.

This particular reviewer, chock full of opinions and suspicions about where the errors and biases in the present analyses are likely to be, goes out on a limb (where a branch belongs) and suggests that when all has been said and done, H_0 from SNe Ia will be in the 50s.

ACKNOWLEDGMENTS

The names of colleagues from whom I have learned about SNe Ia range from Abi to Zalman and would fill a page, but for numerous discussions at the University of Oklahoma, I must thank Eddie Baron, Adam Fisher, and Peter Nugent. Part of this review was written in Trieste during a stimulating visit to the International School of Advanced Studies (SISSA), for which I am indebted to my host, Dennis Sciama. I want to conclude by expressing my appreciation of Allan Sandage and Gustav Tammann for their insights and their perseverance.

<p>Visit the <i>Annual Reviews</i> home page at http://www.AnnualReviews.org.</p>

Literature Cited

- Arnett WD. 1982. Type I supernovae. I. Analytic solutions for the early part of the light curve. *Ap. J.* 253:785–97
- Arnett WD, Branch D, Wheeler JC. 1985. Hubble's constant and exploding carbon-oxygen white dwarf models for Type Ia supernovae. *Nature* 314:337–38
- Arnett WD, Livne E. 1994a. The delayed detonation model of Type Ia supernovae. I. The deflagration phase. *Ap. J.* 427:315–29
- Arnett WD, Livne E. 1994b. The delayed detonation model of Type Ia supernovae. II. The detonation phase. *Ap. J.* 427:330–41
- Barbon R, Benetti S, Cappellaro E, Rosino L, Turatto M. 1990. Type Ia supernova 1989B in NGC 3627. *Astron. Astrophys.* 237:79–90
- Baron E, Hauschildt PH, Nugent P, Branch D. 1996. Non-local thermodynamic equilibrium effects in modeling of supernovae near maximum light. *MNRAS* 283:297–315
- Benz W, Cameron AGW, Bowers RL, Press WH. 1990. Dynamic mass exchange in doubly degenerate binaries. I. 0.9 and 1.2 M_{\odot} stars. *Ap. J.* 348:647–67
- Bowers EJC, Meikle WPS, Geballe TR, Walton NA, Pinto PA, et al. 1997. Infrared and optical spectroscopy of Type Ia supernovae in the nebular phase. *MNRAS* 290:663–79
- Branch D. 1992. The Hubble constant from nickel radioactivity in Type Ia supernovae. *Ap. J.* 392:35–40
- Branch D. 1998. Early-time spectra of Type Ia supernovae and the nature of the peculiar SN 1991T. In *Supernovae and Cosmology*, ed. L Labhardt, B Bingelli, R Buser. Schaub Druck: Sissach. In press
- Branch D, Doggett JB, Nomoto K, Thielemann F-K. 1985. Accreting white dwarf models for Type I supernovae. IV. The optical spectra of carbon deflagration supernovae. *Ap. J.* 294:619–25
- Branch D, Drucker W, Jeffery DJ. 1988. Differences among expansion velocities of Type Ia supernovae. *Ap. J. Lett.* 330:L117–18
- Branch D, Fisher A, Baron E, Nugent P. 1996a. On van den Bergh's method for measuring the Hubble constant from Type Ia supernovae. *Ap. J. Lett.* 470:L7–L9
- Branch D, Fisher A, Herczeg TH, Miller DL, Nugent P. 1994. The distance to the Type Ia supernova 1972E and its parent galaxy NGC 5253: a prediction. *Ap. J. Lett.* 421:L87–L90
- Branch D, Fisher A, Nugent P. 1993. On the relative frequencies of spectroscopically normal and peculiar Type Ia supernovae. *Astron. J.* 106:2383–91
- Branch D, Livio M, Yungelson LR, Boffi FR, Baron E. 1995. In search of the progenitors of Type Ia supernovae. *Publ. Astron. Soc. Pac.* 107:1019–29
- Branch D, Nugent P, Fisher A. 1997. Type Ia supernovae as extragalactic distance indicators. See Ruiz-Lapuente et al. 1997b, pp. 715–34
- Branch D, Romanishin W, Baron E. 1996b. Statistical connections between the properties of Type Ia supernovae and the $B - V$ colors of their parent galaxies, and the value of H_0 . *Ap. J.* 465:73–78
- Branch D, Tammann GA. 1992. Type Ia supernovae as standard candles. *Annu. Rev. Astron. Astrophys.* 30:359–89
- Branch D, van den Bergh S. 1993. Spectroscopic differences between supernovae of Type Ia in early-type and in late-type galaxies. *Astron. J.* 105:2231–35
- Cappellaro E, Mazzali PA, Benetti S, Danziger IJ, Turatto M, et al. 1998. SN Ia light curves and radioactive decay. *Astron. Astrophys.* 328:203–10
- Chiosi C, Wood PR, Capitanio N. 1993. Theoretical models of Cepheid variables and their colors and magnitudes. *Ap. J. Suppl.* 86:541–98
- Colgate SA, Fryer CL, Hand KP. 1997. Low mass SNe Ia and the late light curve. See Ruiz-Lapuente et al. 1997b, pp. 273–302
- Cristiani S, Cappellaro E, Turatto M, Bergeron J, Bues I, et al. 1992. The SN 1986G in Centaurus A. *Astron. Astrophys.* 259:63–70
- Cumming RJ, Lundqvist P, Smith LJ, Pettini M, King DL. 1996. Circumstellar $H\alpha$ from SN 1994D and future Type Ia supernovae: an observational test of progenitor models. *MNRAS* 283:1355–60
- Della Valle M, Panagia N. 1992. Type Ia supernovae in late type galaxies: reddening correction, scale height, and absolute maximum magnitude. *Astron. J.* 104:696–703
- Eastman RG. 1997. Radiation transport in Type Ia supernovae. See Ruiz-Lapuente et al. 1997b, pp. 571–88
- Eck C, Cowan JJ, Roberts D, Boffi FR, Branch D. 1996. Radio observations of the Type Ia supernova 1986G as a test of a symbiotic-star progenitor. *Ap. J. Lett.* 451:L53–L55
- Feast MW, Catchpole RM. 1997. The Cepheid period-luminosity zero-point from Hipparcos trigonometrical parallaxes. *MNRAS* 286:L1–L5
- Filippenko AV. 1997. Optical spectra of supernovae. *Annu. Rev. Astron. Astrophys.* 35:309–55
- Filippenko AV, Richmond MW, Branch D, Gaskell CM, Herbst W, et al. 1992a. The sub-luminous, spectroscopically peculiar Type Ia

- supernova 1991bg in the elliptical galaxy NGC 4374. *Astron. J.* 104:1543–55
- Filippenko AV, Richmond MW, Matheson T, Shields JC, Burbidge EM, et al. 1992b. The peculiar Type Ia SN 1991T: detonation of a white dwarf? *Ap. J.* 384:L15–L18
- Fisher A, Branch D, Höflich PA, Khokhlov A. 1995. The minimum ejection velocity of calcium in Type Ia supernovae and the value of the Hubble constant. *Ap. J. Lett.* 447:L73–L76
- Fisher A, Branch D, Nugent P, Baron E. 1997. Evidence for a high-velocity carbon-rich layer in the Type Ia SN 1990N. *Ap. J. Lett.* 481:L89–L92
- Freedman WL. 1997. Determination of the Hubble constant. In *Critical Dialogues in Cosmology*, ed. N Turok, pp. 92–129. Singapore: World Sci.
- Freedman WL, Madore BF, Kennicutt RC. 1997. Hubble Space Telescope key project on the extragalactic distance scale. See Livio et al, 1997, pp. 171–85
- Garnavich PM, Kirshner RP, Challis P, Tonry J, Gilliland RL, et al. 1998. Constraints on cosmological models from Hubble Space Telescope observations of high- z supernovae. *Ap. J. Lett.* In press
- Goldhaber G, Deustra S, Gabi S, Groom DE, Hook I, et al. 1997. Observations of cosmological time dilation using Type Ia supernovae as clocks. See Ruiz-Lapuente et al, 1997b, pp. 777–84
- Gómez G, López R, Sánchez F. 1996. The Canarias Type Ia supernova archive. *Astron. J.* 112:2094–109
- Gould A. 1994. The metallicity dependence of inferred Cepheid distances. *Ap. J.* 426:542–52
- Hachisu I, Kato M, Nomoto K. 1996. A new model for progenitor systems of Type Ia supernovae. *Ap. J. Lett.* 470:L97–100
- Hamuy M, Maza J, Phillips MM, Suntzeff NB, Wischnjewsky M, et al. 1993. The 1990 Calán/Tololo supernova search. *Astron. J.* 106:2392–407
- Hamuy M, Phillips MM, Maza J, Suntzeff NB, Della Valle M, et al. 1995a. SN 1992K: a twin to the subluminous Type Ia SN 1991bg. *Astron. J.* 108:2226–32
- Hamuy M, Phillips MM, Maza J, Wischnjewsky M, Uomoto A, et al. 1991. The optical light curves of SN 1980N and SN 1981D in NGC 1316 (Fornax A). *Astron. J.* 102:208–17
- Hamuy M, Phillips MM, Schommer RA, Suntzeff NB, Maza J, Avilés R. 1996a. The absolute luminosities of the Calán/Tololo Type Ia supernovae. *Astron. J.* 112:2391–97
- Hamuy M, Phillips MM, Suntzeff NB, Schommer RA, Maza J, Avilés R. 1995b. A Hubble diagram of distant supernovae. *Astron. J.* 109:1–13
- Hamuy M, Phillips MM, Suntzeff NB, Schommer RA, Maza J, Avilés R. 1996b. The Hubble diagram of the Calán/Tololo Type Ia supernovae and the value of H_0 . *Astron. J.* 112:2398–407
- Hamuy M, Phillips MM, Suntzeff NB, Schommer RA, Maza J, et al. 1996c. *BVRI* light curves for 29 Type Ia supernovae. *Astron. J.* 112:2408–37
- Hamuy M, Phillips MM, Suntzeff NB, Schommer RA, Maza J, et al. 1996d. The morphology of Type Ia supernova light curves. *Astron. J.* 112:2438–47
- Harkness R. 1991a. A comparison of carbon deflagration models for SNe Ia. In *Supernovae*, ed. SE Woosley, pp. 454–63. New York: Springer
- Harkness R. 1991b. Type Ia supernovae. In *SN 1987A and Other Supernovae*, ed. IJ Danziger, K Kjær, pp. 447–56. Dordrecht: Kluwer
- Hatano K, Deaton J, Branch D. 1998. *Ap. J. Lett.* In press
- Ho LC, Filippenko AV. 1995. Probing the interstellar medium along the lines of sight to supernovae 1994D and 1994I. *Ap. J.* 444:165–74; Erratum: 463:818
- Höflich P. 1995. Analysis of the Type Ia supernova 1994D. *Ap. J.* 443:89–108
- Höflich P, Khokhlov A. 1996. Explosion models for Type Ia supernovae: a comparison with observed light curves, distances, H_0 , and q_0 . *Ap. J.* 457:500–28
- Höflich P, Khokhlov A, Müller E. 1992. Gamma-ray light curves and spectra of Type Ia supernovae. *Astron. Astrophys.* 259:549–66
- Höflich P, Khokhlov A, Müller E. 1993. Light curve models for Type Ia supernovae: physical assumptions, their influence and validity. *Astron. Astrophys.* 268:570–90
- Höflich P, Khokhlov A, Wheeler JC, Nomoto K, Thielemann F-K. 1997. Explosion models, light curves, spectra, and H_0 . See Ruiz-Lapuente et al, 1997b, pp. 659–79
- Höflich P, Khokhlov A, Wheeler JC, Phillips MM, Suntzeff NB, Hamuy M. 1996. Maximum brightness and postmaximum decline of light curves of Type Ia supernovae: a comparison of theory and observations. *Ap. J.* 472:L81–L84
- Iben II. 1997. Scenarios for Type Ia supernovae. See Ruiz-Lapuente et al, 1997b, pp. 111–26
- Iben II, Tutukov AV. 1984. Supernovae of Type I as end products of the evolution of binaries with components of moderate initial mass ($M \leq 9 M_\odot$). *Ap. J. Suppl.* 54:335–72
- Jacoby GH, Pierce MJ. 1996. Response to Schaefer's comments on Pierce & Jacoby

- (1995) regarding the Type Ia supernova 1937C. *Astron. J.* 112:723–31
- Jeffery DJ, Leibundgut B, Kirshner RP, Benetti S, Branch D, Sonneborn G. 1992. Analysis of the photospheric epoch spectra of Type Ia supernovae 1990N and 1991T. *Ap. J.* 397:304–28
- Kennicutt RC, Stetson PB, Saha A, Kelson D, Rawson D, et al. 1998. The *HST* key project on the extragalactic distance scale XIII. The metallicity dependence of the Cepheid distance scale. *Ap. J.* In press
- Khokhlov A, Müller E, Höflich P. 1993. Light curves of Type Ia supernova models with different explosion mechanisms. *Astron. Astrophys.* 270:223–48
- Kim AG, Gabi S, Goldhaber G, Groom DE, Hook IM, et al. 1997. Implications for the Hubble constant from the first seven supernovae at $z \geq 0.35$. *Ap. J. Lett.* 476:L63–66
- Kirshner RP, Jeffery DJ, Leibundgut B, Sonneborn G, Phillips MM, et al. 1993. SN 1992A: ultraviolet and optical observations based on HST, IUE, and CTIO observations. *Ap. J.* 415:589–615
- Kochanek CS. 1997. Rebuilding the Cepheid distance scale. I. A global analysis of Cepheid mean magnitudes. *Ap. J.* 491:13–28
- Leibundgut B, Kirshner RP, Filippenko AV, Shields JC, Foltz CB, et al. 1991a. Premaximum observations of the Type Ia SN 1990N. *Ap. J. Lett.* 371:L23–26
- Leibundgut B, Kirshner RP, Phillips MM, Wells LA, Suntzeff NB, et al. 1993. SN 1991bg: a Type Ia supernova with a difference. *Astron. J.* 105:301–13
- Leibundgut B, Schommer R, Phillips MM, Riess A, Schmidt B, et al. 1996. Time dilation in the light curve of the distant Type Ia supernova 1995K. *Ap. J. Lett.* 466:L21–L24
- Leibundgut B, Tammann GA, Cadonau R, Cerreto D. 1991b. Supernova studies. VII. An atlas of the light curves of supernovae Type I. *Astron. Astrophys. Suppl.* 89:537–79
- Li X-D, van den Heuvel EPJ. 1997. Evolution of white dwarf binaries: supersoft X-ray sources and progenitors of Type Ia supernovae. *Astron. Astrophys.* 322:L9–12
- Lira P. 1996. *Light curves of the supernovae 1990N and 1991T*. MS thesis. Univ. Chile
- Lira P, Suntzeff NB, Phillips MM, Hamuy M, Maza J, et al. 1998. Optical light curves of the Type Ia supernovae 1990N and 1991T. *Astron. J.* 115:234–46
- Liu W, Jeffery DJ, Schultz DR. 1997a. Nebular spectra of Type Ia supernovae. *Ap. J. Lett.* 483:L107–10
- Liu W, Jeffery DJ, Schultz DR. 1997b. Nebular spectra of the unusual Type Ia supernova 1991T. *Ap. J. Lett.* 486:L35–38
- Liu W, Jeffery DJ, Schultz DR, Quinet P, Shaw J, Pindzola MS. 1997c. Emission from cobalt in type Ia supernovae. *Ap. J. Lett.* 489:L141–43
- Livio M, Donahue M, Panagia N, eds. 1997. *The Extragalactic Distance Scale*. Cambridge: Cambridge Univ. Press
- Livne E. 1990. Successive detonations in accreting white dwarfs as an alternative mechanism for Type Ia supernovae. *Ap. J.* 354:L53–55
- Livne E, Arnett WD. 1995. Explosions of sub-Chandrasekhar mass white dwarfs in two dimensions. *Ap. J.* 452:62–74
- Lundqvist P, Cumming RJ. 1997. Supernova progenitor constraints from circumstellar interaction: Type Ia. In *Advances in Stellar Evolution*, ed. RT Rood, A Renzini, pp. 293–97. Cambridge: Cambridge Univ. Press
- Madore BF, Freedman WL. 1991. The Cepheid distance scale. *Publ. Astron. Soc. Pac.* 103:933–57
- Madore BF, Freedman WL. 1998. Hipparcos parallaxes and the Cepheid distance scale. *Ap. J. Lett.* 492:110–15
- Mazzali PA, Chugai N, Turatto M, Lucy LB, Danziger IJ, et al. 1997. The properties of the peculiar Type Ia supernova 1991bg. II. The amount of ^{56}Ni and the total ejecta mass determined from spectrum synthesis and energetics considerations. *MNRAS* 284:151–71
- Mazzali PA, Danziger IJ, Turatto M. 1995. A study of the properties of the peculiar SN Ia 1991T through models of its evolving early-time spectra. *Astron. Astrophys.* 297:509–34
- Mazzali PA, Lucy LB, Danziger IJ, Gouiffes C, Cappellaro E, Turatto M. 1993. Models for the early-time spectral evolution of the standard type Ia supernova 1990N. *Astron. Astrophys.* 269:423–45
- Meikle WPS, Cumming RJ, Geballe TR, Lewis JR, Walton NA, et al. 1996. An early-time infrared and optical study of the Type Ia supernovae 1994D and 1991T. *MNRAS* 281:263–80
- Milne PA, The L-S, Leising MD. 1998. Is positron escape seen in the light curves of Type Ia supernovae? *Ap. J.* In press
- Minkowski R. 1939. The spectra of the supernovae in IC 4182 and NGC 1003. *Ap. J.* 89:156–217
- Mochkovitch R, Guerrero J, Segretain L. 1997. The merging of white dwarfs. See Ruiz-Lapuente et al, 1997b, pp. 187–204
- Mochkovitch R, Livio M. 1990. The coalescence of white dwarfs and Type I supernovae. The merged configuration. *Astron. Astrophys.* 236:378–84
- Nomoto K, Iwamoto K, Nakasato N, Thielemann F-K, Brachwitz F, et al. 1997. Type Ia supernovae: progenitors and constraints on nucleosynthesis. See Ruiz-Lapuente et al 1997b, pp. 349–78

- Nomoto K, Thielemann F-K, Yokoi K. 1984. Accreting white dwarf models for Type Ia supernovae. III. Carbon deflagration supernovae. *Ap. J.* 286:644–58
- Nugent P, Baron E, Branch D, Fisher A, Hauschildt PH. 1997. Synthetic spectra of hydrodynamical models of Type Ia supernovae. *Ap. J.* 485:812–19
- Nugent P, Baron E, Hauschildt PH, Branch D. 1995a. Spectrum synthesis of the Type Ia supernovae 1992A and 1981B. *Ap. J.* 441:L33–36
- Nugent P, Branch D, Baron E, Fisher A, Vaughan TE, Hauschildt PH. 1995b. Low Hubble constant from the physics of Type Ia supernovae. *Phys. Rev. Lett.* 75:394–97; Erratum: 75:1874
- Nugent P, Phillips M, Baron E, Branch D, Hauschildt PH. 1995c. Evidence for a spectroscopic sequence among Type Ia supernovae. *Ap. J. Lett.* 455:L147–50
- Patat F, Barbon R, Cappellaro E, Turatto M. 1997. Revised photometry and color distribution of Type Ia supernovae observed at Asiago in the seventies. *Astron. Astrophys.* 317:423–31
- Patat F, Benetti S, Cappellaro E, Danziger IJ, Della Valle M, et al. 1996. The Type Ia supernova 1994D in NGC 4526: the early phases. *MNRAS* 278:111–24
- Pauldrach AWA, Duschinger M, Mazzali PA, Puls J, Lennon M, Miller DL. 1996. NLTE models for synthetic spectra of Type Ia supernovae. *Astron. Astrophys.* 312:525–38
- Perlmutter S, Aldering G, Della Valle M, Deustua S, Ellis RS, et al. 1998. Discovery of a supernova explosion at half the age of the Universe and its cosmological implications. *Nature* 391:51–54
- Perlmutter S, Deustua S, Goldhaber G, Groom D, Hook I, et al. 1997a. *Supernovae. IAU Circ.* No. 6621
- Perlmutter S, Gabi S, Goldhaber S, Groom DE, Hook IM, et al. 1997b. Measurements of the cosmological parameters Ω and Λ from the first seven supernovae at $z \geq 0.35$. *Ap. J.* 483:565–81
- Phillips MM. 1993. The absolute magnitudes of Type Ia supernovae. *Ap. J. Lett.* 413:L105–8
- Phillips MM, Phillips AC, Heathcote SR, Blanco VM, Geisler D. 1987. The Type Ia supernova 1986G in NGC 5128: optical photometry and spectroscopy. *Publ. Astron. Soc. Pac.* 99:592–605
- Phillips MM, Wells LA, Suntzeff NB, Hamuy M, Leibundgut B, et al. 1992. SN 1991T: further evidence of the heterogeneous nature of Type Ia supernovae. *Astron. J.* 103:1632–37
- Pierce MJ, Jacoby GH. 1995. “New” B and V photometry of the “old” Type Ia supernova 1937C: implications for H_0 . *Astron. J.* 110:2885–909
- Pinto PA. 1997. Time dependence and the opacity of Type Ia supernovae. See Ruiz-Lapuente et al. 1997b, pp. 607–25
- Pskovskii YP. 1977. Brightness, color, and expansion velocity of SNe I as functions of the rate of brightness decline. *Sov. Astron. AJ.* 21:675
- Rappaport SA, Di Stefano R, Smith M. 1994. Formation and evolution of supersoft X-ray sources. *Ap. J.* 426:692–703
- Rasio FA, Shapiro SL. 1995. Hydrodynamics of binary coalescence. II. Polytropes with $\Gamma = 5/3$. *Ap. J.* 438:887–903
- Renzini A. 1996. Searching for Type Ia supernova progenitors. In *Supernovae and Supernova Remnants*, ed. R McCray, Z Wang, pp. 77–85. Cambridge: Cambridge Univ. Press
- Richmond MW, Treffers RR, Filippenko AV, Van Dyk SD, Paik Y, et al. 1995. *UBVRI* photometry of the Type Ia SN 1994D in NGC 4526. *Astron. J.* 109:2121–33
- Riess AG. 1996. *Type Ia supernova multicolor light curve shapes*. PhD thesis. Harvard Univ.
- Riess AG, Davis M, Baker J, Kirshner RP. 1997a. The velocity field from Type Ia supernovae matches the gravity field from galaxy surveys. *Ap. J.* 488:L1–L5
- Riess AG, Filippenko AV, Leonard DC, Schmidt BP, Suntzeff N, et al. 1997b. Time dilation from spectral feature age measurements of Type Ia supernovae. *Astron. J.* 114:722–29
- Riess AG, Nugent P, Filippenko AV, Kirshner RP, Perlmutter S. 1998. Snapshot distances to SNe Ia—all in “one” night’s work. *Ap. J.* In press
- Riess AG, Press WH, Kirshner RP. 1995a. Using Type Ia supernova light curve shapes to measure the Hubble constant. *Ap. J. Lett.* 438:L17–20
- Riess AG, Press WH, Kirshner RP. 1995b. Determining the motion of the local group using Type Ia supernova light curve shapes. *Ap. J. Lett.* 445:L91–94
- Riess AG, Press WH, Kirshner RP. 1996a. A precise distance indicator: Type Ia supernova multicolor light-curve shapes. *Ap. J.* 473:88–109
- Riess AG, Press WH, Kirshner RP. 1996b. Is the dust obscuring supernovae in distant galaxies the same as the dust in the Milky Way? *Ap. J.* 473:588–94
- Ruiz-Lapuente P. 1996. The Hubble constant from ^{56}Co -powered nebular candles. *Ap. J.* 465:L83–86
- Ruiz-Lapuente P, Canal R, Burkert A. 1997a. SNe Ia: on the binary progenitors and expected statistics. See Ruiz-Lapuente et al. 1997b, pp. 205–30
- Ruiz-Lapuente P, Canal R, Isern J, eds. 1997b.

- Thermonuclear Supernovae*. Dordrecht: Kluwer
- Ruiz-Lapuente P, Cappellaro E, Turatto M, Gouiffes C, Danziger IJ, et al. 1992. Modeling the iron-dominated spectra of the Type Ia supernova 1991T at premaximum. *Ap. J. Lett.* 387:L33–36
- Saha A, Labhardt L, Schwengeler H, Macchetto FD, Panagia N, et al. 1994. Discovery of Cepheids in IC 4182: absolute peak brightness of SN Ia 1937C and the value of H_0 . *Ap. J.* 425:14–34
- Saha A, Sandage A, Labhardt L, Schwengeler H, Tammann GA, et al. 1995. Discovery of Cepheids in NGC 5253: absolute peak brightness of SNe Ia 1895B and 1972E and the value of H_0 . *Ap. J.* 438:8–26
- Saha A, Sandage A, Labhardt L, Tammann GA, Macchetto FD, Panagia N. 1996a. Cepheid calibration of the peak brightness of SNe Ia. V. SN 1981B in NGC 4536. *Ap. J.* 466:55–91
- Saha A, Sandage A, Labhardt L, Tammann GA, Macchetto FD, Panagia N. 1996b. Cepheid calibration of the peak brightness of Type Ia supernovae. VI. SN 1960F in NGC 4496A. *Ap. J. Suppl.* 107:693
- Saha A, Sandage A, Labhardt L, Tammann GA, Macchetto FD, Panagia N. 1997. Cepheid calibration of the peak brightness of Type Ia supernovae. VII. SN 1990N in NGC 4639. *Ap. J.* 486:1–20
- Saio H, Gautschy A. 1998. On the theoretical period-luminosity relations of Cepheids. *Ap. J.* In press
- Sandage A. 1996. Annual report of the Carnegie Observatories. *BAAS* 28(1):52
- Sandage A, Saha A, Tammann GA, Panagia N, Macchetto FD. 1992. The Cepheid distance to IC 4182; calibration of M_V for SN Ia 1937C and the value of H_0 . *Ap. J. Lett.* 401:L7–10
- Sandage A, Tammann GA. 1982. Steps toward the Hubble constant. VIII. The global value. *Ap. J.* 256:339–45
- Sandage A, Tammann GA. 1993. The Hubble diagram in V for supernovae of Type Ia and the value of H_0 therefrom. *Ap. J.* 415:1–9
- Sandage A, Tammann GA. 1997. The evidence for the long distance scale with $H_0 < 65$. In *Critical Dialogues in Cosmology*, ed. N Turok, pp. 130–55. Singapore: World Sci.
- Sandage A, Tammann GA. 1998. Confirmation of previous ground-based Cepheid P-L zero-points using Hipparcos trigonometric parallaxes. *MNRAS* In press
- Sasselov DD, Beaulieu JP, Renault C, Grison P, Ferlet R, et al. 1997. Metallicity effects on the Cepheid extragalactic distance scale from EROS photometry in the Large Magellanic Cloud and the Small Magellanic Cloud. *Astron. Astrophys.* 324:471–82
- Schaefer BE. 1994. The peak brightness of SN 1937C in IC 4182 and the Hubble constant. *Ap. J.* 426:493–501
- Schaefer BE. 1995a. The peak brightness of SN 1895B in NGC 5253 and the Hubble constant. *Ap. J. Lett.* 447:L13–16
- Schaefer BE. 1995b. The peak brightness of supernovae in the U band and the Hubble constant. *Ap. J. Lett.* 450:L5–9
- Schaefer BE. 1995c. The peak brightness of SN 1981B in NGC 4536 and the Hubble constant. *Ap. J. Lett.* 449:L9–12
- Schaefer BE. 1996a. The peak brightness of SN 1937C and the Hubble constant: comments on Pierce & Jacoby (1995). *Astron. J.* 111:1668–74
- Schaefer BE. 1996b. The peak brightness of SN 1960F in NGC 4496 and the Hubble constant. *Ap. J. Lett.* 460:L19–23
- Schlegel EM, Petre R. 1993. A *ROSAT* upper limit on X-ray emission from SN 1992A. *Ap. J. Lett.* 412:L29–32
- Schmidt B, Phillips M, Hamuy M, Avilés R, Suntzeff N, et al. 1997. *Supernovae*. *IAU Circ.* No. 6646
- Shigeyama T, Nomoto K, Yamaoka H, Thielemann F-K. 1992. Possible models for the type Ia supernova 1990N. *Ap. J. Lett.* 386:L13–16
- Stothers RB. 1988. Abundance effects on the Cepheid distance scale. *Ap. J.* 329:712–19
- Tammann GA, Federspiel M. 1997. Focusing in on H_0 . See Livio et al. 1997, pp. 137–70
- Tammann GA, Sandage A. 1995. The Hubble diagram for supernovae of Type Ia. II. The effects on the Hubble constant of a correlation between absolute magnitude and light curve decay rate. *Ap. J.* 452:16–24
- Teerikorpi P. 1997. Observational selection bias affecting the determination of the extragalactic distance scale. *Annu. Rev. Astron. Astrophys.* 35:101–36
- Tripp R. 1997. Using distant Type Ia supernovae to measure the cosmological expansion parameters. *Astron. Astrophys.* 325:871–76
- Tripp R. 1998. A two-parameter luminosity correction for Type Ia supernovae. *Astron. Astrophys.* In press
- Turatto M, Benetti S, Cappellaro E, Danziger IJ, Della Valle M, et al. 1996. The properties of the peculiar Type Ia supernova 1991bg. I. Analysis and discussion of two years of observations. *MNRAS* 283:1–17
- Tutukov A, Yungelson LR. 1994. Merging of binary white dwarfs, neutron stars, and black holes under the influence of gravitational wave radiation. *MNRAS* 268:871–79
- Vacca WD, Leibundgut B. 1996. The rise times and bolometric light curve of SN 1994D: constraints on models of Type Ia supernovae. *Ap. J. Lett.* 471:L37–40
- van den Bergh S. 1995. A new method for the

- determination of the Hubble parameter. *Ap. J. Lett.* 453:L55–56
- van den Bergh S. 1996. The luminosities of supernovae of Type Ia derived from Cepheid calibrations. *Ap. J.* 472:431–34
- van den Heuvel EPJ, Bhattacharya D, Nomoto K, Rappaport SA. 1992. Accreting white dwarf models for CAL83, CAL87, and other ultrasoft X-ray sources in the LMC. *Astron. Astrophys.* 262:97–105
- Vaughan TE, Branch D, Miller DL, Perlmutter S. 1995. The blue and visual absolute magnitude distributions of Type Ia supernovae. *Ap. J.* 439:558–64
- von Hippel T, Bothun GD, Schommer RA. 1997. Stellar populations and the white dwarf mass function: connections to supernova Ia luminosities. *Astron. J.* 114:1154–64
- Wang L, Höflich P, Wheeler JC. 1997a. Supernovae and their host galaxies. *Ap. J.* 483:L29–L32
- Wang L, Wheeler JC, Höflich P. 1997b. Polarimetry of the Type Ia supernova 1996X. *Ap. J.* 476:L27–30
- Wang L, Wheeler JC, Li Z, Clocchiatti A. 1996. Broadband polarimetry of supernovae: 1994D, 1994Y, 1994ae, 1995D, and 1995H. *Ap. J.* 467:435–45
- Wells LA, Phillips MM, Suntzeff NB, Heathcote SR, Hamuy M, et al. 1994. The Type Ia supernova 1989B in NGC 3627 (M66). *Astron. J.* 108:2233–50
- Wheeler JC, Harkness RP, Khokhlov AM, Höflich P. 1995. Stirling’s supernovae: a survey of the field. *Phys. Rep.* 256:211–35
- Woosley SE, Weaver TA. 1986. The physics of supernova explosions. *Annu. Rev. Astron. Astrophys.* 24:205–53
- Woosley SE, Weaver TA. 1994a. Sub-Chandrasekhar models for Type Ia supernovae. *Ap. J.* 423:371–79
- Woosley SE, Weaver TA. 1994b. Massive stars, supernovae, and nucleosynthesis. In *Supernovae*, ed. S Bludman, R Mochkovitch, J Zinn-Justin, pp. 63–154. Amsterdam: Elsevier
- Yungelson LR, Livio M. 1998. Type Ia supernovae: an examination of potential progenitors and the redshift distribution. *Ap. J.* In press
- Yungelson LR, Livio M, Truran JW, Tutukov A, Fedorova A. 1996. A model for the Galactic population of binary supersoft X-ray sources. *Ap. J.* 466:890–910
- Zehavi I, Riess AG, Kirshner RP, Dekel A. 1998. A local Hubble bubble from SNe Ia? *Ap. J.* In press